Geochemistry, Geophysics, Geosystems®

RESEARCH ARTICLE
10.1029/2025GC012177

Key Points:

- Three spatially distinct groups of N_2-dominated, CO_2-dominated and H_2S-rich gases
- Significant geogenic CO_2 degassing of dominant crustal origin
- Up to 25% of mantle helium contribution

Supporting Information:

Supporting Information may be found in the online version of this article.

Correspondence to:

L. Li Vigni and M. Temovski,
lorenza.livigni@unipa.it;
temovski.marjan@atomki.hu

Citation:

Li Vigni, L., Temovski, M., Cardellini, C., Molnár, K., Ionescu, A., Mirčovski, V., et al. (2025). Toward solving the mystery of elevated tectonic degassing in South Eastern Europe: Insights from gas discharges along the Vardar suture (North Macedonia). *Geochemistry, Geophysics, Geosystems*, *26*, e2025GC012177. https://doi.org/10.1029/2025GC012177

Received 14 JAN 2025
Accepted 12 JUN 2025

Author Contributions:

Conceptualization: L. Li Vigni, M. Temovski, W. D'Alessandro
Data curation: L. Li Vigni, M. Temovski, W. D'Alessandro
Funding acquisition: M. Temovski, C. Cardellini, W. D'Alessandro
Investigation: L. Li Vigni, M. Temovski, K. Molnár, A. Ionescu, W. D'Alessandro
Supervision: M. Temovski, C. Cardellini, W. D'Alessandro
Writing – original draft: L. Li Vigni, M. Temovski, W. D'Alessandro
Writing – review & editing: L. Li Vigni, M. Temovski, C. Cardellini, K. Molnár, A. Ionescu, V. Mirčovski,

Toward Solving the Mystery of Elevated Tectonic Degassing in South Eastern Europe: Insights From Gas Discharges Along the Vardar Suture (North Macedonia)

L. Li Vigni[1,2], M. Temovski[3,4], C. Cardellini[5,6], K. Molnár[3], A. Ionescu[5,7,8], V. Mirčovski[9], K. Daskalopoulou[10], G. Chiodini[6], F. Parello[1,2], and W. D'Alessandro[2]

[1]Dipartimento Scienze della Terra e del Mare, Università di Palermo, Palermo, Italy, [2]Istituto Nazionale di Geofisica e Vulcanologia (INGV) – Sezione di Palermo, Palermo, Italy, [3]Isotope Climatology and Environmental Research Centre, HUN-REN Institute for Nuclear Research (ATOMKI), Debrecen, Hungary, [4]Department of Mineralogy and Geology, University of Debrecen, Debrecen, Hungary, [5]Dipartimento di Fisica e Geologia, Università di Perugia, Perugia, Italy, [6]Istituto Nazionale di Geofisica e Vulcanologia (INGV) – Sezione di Bologna, Naples, Italy, [7]Faculty of Environmental Science and Engineering, Babes-Bolyai University, Cluj-Napoca, Romania, [8]Faculty of Biology and Geology, Babes-Bolyai University, Cluj-Napoca, Romania, [9]Faculty of Natural and Technical Sciences, Goce Delčev University, Štip, North Macedonia, [10]University of Potsdam, Institute of Geosciences, Potsdam-Golm, Germany

Abstract Tectonic carbon degassing is an important contributor to the global carbon cycle. South Eastern Europe is an active extensional tectonic region. This is the result of intense geodynamic events related to the closure of the Tethys Ocean, whose remnants include an ophiolite orogenic belt and the Vardar megasuture. In North Macedonia, regional active fault systems, seismic activity, Cenozoic-Quaternary volcanism, large-scale degassing, and low-enthalpy geothermal resources are widespread. Nonetheless, a geochemical characterization of the gas manifestations is missing from the literature. Toward this contribution, we report the first characterization of chemical and isotopic compositions of fluids from the main geothermal and cold gas manifestations of North Macedonia, and we explore their origins, the processes controlling their chemistry, and their relationships with the regional geodynamic situation. Gas samples were collected along the whole country, and were analyzed for both their chemical (He, H_2, H_2S, O_2, N_2, CO_2, CH_4, Ar) and isotopic composition ($\delta^{13}C$-CO_2, He, Ar). Based on their chemistry, samples can be subdivided into three groups: (a) N_2-dominated, (b) CO_2-dominated, and (c) H_2S-rich, which are geographically well separated, following regional distributions. The CO_2-dominated group is the most widespread, highlighting the importance of geogenic carbon degassing in the study area. Its origin is prevailingly crustal ($\delta^{13}C$-CO_2 = −4.6–+1.0‰ vs. V-PDB; R/R_A = 0.1–1.8), but a significant, up to 25%, mantle contribution can be inferred from the He isotope composition.

Plain Language Summary The Earth emits a considerable quantity of deep gases, especially carbon dioxide, not only from the most well-known volcanic systems but also from structural systems, such as active fault systems that can generate earthquakes. The Balkan Peninsula is an area rich in degassing structural systems, which have not been as extensively studied as other areas. The objective of this study was to investigate the degassing manifestation in North Macedonia. This is the first study to examine the composition of the gases in order to ascertain their origin, the processes controlling their chemistry, and their relationship with the structural systems of the area. The samples can be classified into three groups based on the most abundant gas species: (a) N_2-dominated, (b) CO_2-dominated, and enrichments (c) H_2S-rich. These groups are geographically well separated and located in the eastern, central and western parts of the country, respectively. The CO_2-dominated group is the most widespread. This finding further highlights the importance of carbon degassing in the Balkan Peninsula. Carbon in the area predominantly derives from the crust, although evidence suggests a significant mantle contribution, as indicated by the helium isotope composition.

1. Introduction

During the last decades, scientific research concerning the estimation of endogenous carbon degassing into the atmosphere has sharply increased due to the major role of this element in controlling the Earth's climate over geological time (Foster et al., 2017). Among the greenhouse gases, carbon dioxide and methane are considered to be the most effective species in contributing to the changing of the global climate. The most recent observations from the NOAA Mauna Loa Observatory, updated to June 2024, report a mean abundance of CO_2 and CH_4 of

K. Daskalopoulou, G. Chiodini, F. Parello, W. D'Alessandro

426.9 ppm and 1,931 ppb, respectively, in the atmosphere (https://gml.noaa.gov/ccgg/trends/). In comparison, the global mean abundance in 2022 was estimated at 417.9 ± 0.2 ppm for CO_2 and at 1,923 ± 2 ppb for CH_4 (Nineteenth WMO Greenhouse Gas Bulletin, 2023), with an increment of about 3% with respect to the observations of 2018 reported in the Fifteenth WMO Greenhouse Gas Bulletin, 2019 (CO_2 = 407.8 ± 0.1 ppm; CH_4 1,869 ± 2 ppb).

Despite a significant improvement in the worldwide data set, the global flux of CO_2 degassing from the Earth's interior is still the least well-quantified part of the global cycle (Berner & Lasaga, 1989). Many studies have been devoted to the quantification of the release of geogenic CO_2 to the atmosphere from different geological settings (e.g., Brune et al., 2017; Kerrick, 2001; Mörner & Etiope, 2002), and most of them have focused on the present-day CO_2 emission from volcanoes (Brantley & Koepenick, 1995; Burton et al., 2013; Werner et al., 2019). While the volcanic carbon budget is the most studied, its quantification is still far from being well defined. Fischer et al. (2019) estimated a global volcanic CO_2 flux budget of 51.3 ± 5.7 Tg a^{-1} for weakly emitting volcanoes and 1.8 ± 0.9 Tg a^{-1} for eruptive degassing during the 2005–2015 period.

Although the close relationship between tectonically active areas, fluid migration, and geogenic diffuse carbon emissions has long been evidenced (Barnes et al., 1978; Irwin & Barnes, 1980), only in the last decades has tectonic carbon degassing been emphasized as an important contribution to the global carbon cycle (e.g., Chiodini et al., 1999, 2000, 2011; D'Alessandro et al., 2020; Daskalopoulou et al., 2019; Frondini et al., 2019; Kerrick et al., 1995; Lewicki & Brantley, 2000; Li Vigni et al., 2022; Randazzo et al., 2021, 2022; Seward & Kerrick, 1996; Yuçe et al., 2017). At a global scale, the geographic distribution and the amount of deeply derived fluids are controlled by regional normal/transcurrent faulting (Tamburello et al., 2018) and continental rift lengths (Brune et al., 2017). Deep fault systems, due to their enhanced permeability and porosity, play an important role in the transfer of deeply derived volatiles (e.g., CO_2 and He). They create preferential pathways for advective gas-carrying fluids rising from the deep crust or the mantle to the Earth's surface (Caracausi & Sulli, 2019; Faulker et al., 2010; Hunt et al., 2017; Muirhead et al., 2016; Tamburello et al., 2018). The fluid flow, along regional fractures, has been observed to be rapid, with velocities ranging from 10^{-6} to 10^{-5} ms^{-1}, and relatively short-lived, with a duration in the order of a few hundreds of years (John et al., 2012; Kleine et al., 2016). Eventually, fluids and their corresponding volatiles escape through the soil into the atmosphere as a result of pressure decrease (King, 1986). Furthermore, these geogenic fluids play an active role in deep earthquake generation (Buttita et al., 2020; Caracausi et al., 2022; Chiodini et al., 2020; Du et al., 2006; Miller et al., 1999).

In South Eastern Europe (e.g., Balkan Peninsula), large-scale degassing of mantle-derived carbon, Cenozoic volcanism, seismic activity, and regional active fault systems are widespread (Burchfiel et al., 2008; Cvetkovic et al., 2016; Dumurdzanov et al., 2005; Jolivet & Brun, 2010). However, the estimation of endogenous CO_2 release from this area remains poorly quantified (D'Alessandro et al., 2020; Daskalopoulou et al., 2019; Lévy et al., 2023; Li Vigni et al., 2022; Kis et al., 2017, 2019; Minissale et al., 2023; Randazzo et al., 2021). North Macedonia belongs to the South Balkan extensional region (Dumurdzanov et al., 2005) and is considered one of the richest regions in low-temperature geothermal resources (Popovska-Vasilevska & Armenski, 2016). Indeed, the Macedonian region is characterized by positive geothermal anomalies (60–120 mW m^{-2}; Gorgieva et al., 2000; Milivojevic, 1993), which together with crustal thinning favored the occurrence of 18 geothermal fields (Figure S1 in Supporting Information S1), whose surface expressions are more than 50 mineral and thermo-mineral springs (Gorgieva et al., 2000; Popovska-Vasilevska & Armenski, 2016).

Since ancient times, these geothermal systems have been used for balneology purposes as spas, with ruins of Roman and Turkish baths found near some of these thermal springs. Nowadays, the geothermal resources are also used for heating hotels and greenhouses, CO_2 extraction, or industrial utilization, whilst some discharges are without any use.

The geochemical characterization of these gas manifestations and the estimation of their outgassing rate have remained poorly studied and mainly focused on the Duvalo degassing system (Iloski et al., 1957; Li Vigni et al., 2022; Markoski et al., 2019; Trojanović, 1925). The present study reports, for the first time, the chemical and isotopic compositions of fluids (gases in both free and dissolved phase) released from the main geothermal and cold gas manifestations of North Macedonia. This research explores (a) the fluid sources, (b) the processes controlling the fluid chemistry, and (c) the relationships with the regional geodynamic situation of the area.

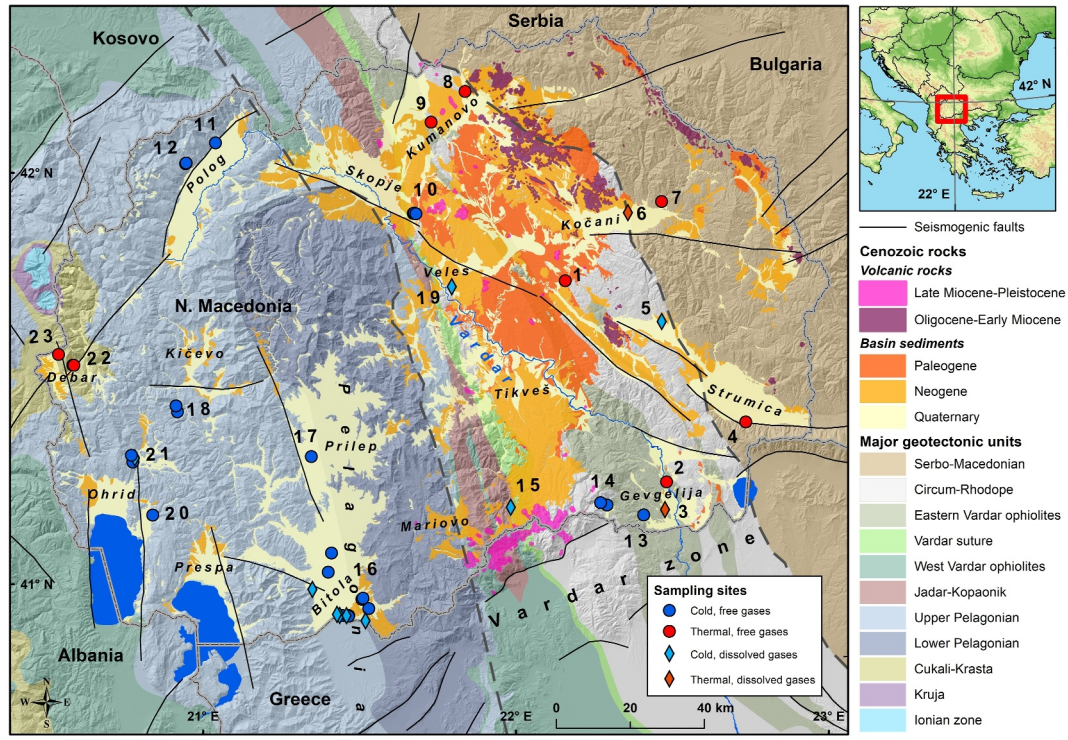

Figure 1. Location of the sampled sites: 1—Kežovica, 2—Smokvica, 3—Negorci, 4—Bansko, 5—Rakliš, 6—Dobra, 7—Istibanja, 8—Strnovac Banja, 9—Kumanovska Banja, 10—Katlanovo, 11—Lešok, 12—Banjiče, 13—Gorničet, 14—Smrdliva Voda and Makedonska Češma, 15—Topli Dol, 16—Bitola basin sites (Geogas, Logovardi, Kisela Voda, Medžitlija, Bitola, Bitola 2, Pelagonka, Pela Rosa, Germijan, Busemak, Gneotino 1, Gneotino 2), 17—Krušeani, 18—Svinjište and Kozica, 19—Sabotna Voda, 20—Duvalo (Kosel), 21—Botun, Petkoniva and Kiselo Klajnče, 22—Kosovrasti, 23—Banjište. Main geotectonic units from Schmid et al. (2020). Extension of Cenozoic sediments after Dumurdzanov et al. (2004, 2005) and volcanic rocks after Molnár et al. (2022). Seismogenic crustal faults from the European Database of Seismogenic Faults (EDSF; https://edsf13.ingv.it/). Dashed black lines approximate the extent of the Vardar zone. Extensional basins and geothermal fields mentioned in the text are also indicated.

2. Geological Settings

North Macedonia, in the central part of the Balkan Peninsula, is located at the junction of the Dinarides-Hellenides and Carpatho-Balkanides orogens, which were formed due to the convergence of the Adriatic microplate and the European plate (Figure 1). This led to the closure of the Neotethys in Late Cretaceous times, marked by the Vardar suture zone. Adria-derived units (e.g., Pelagonian massif, West-Macedonian zone) and obducted Western Vardar ophiolites are found west of the suture zone, while the area to the east is composed of Europe-derived units (e.g., Serbo-Macedonian massif, Circum-Rhodope), as well as Eastern Vardar ophiolites (Schmid et al., 2020). The wider area along the Vardar suture zone between the Dinarides-Hellenides and Carpatho-Balkanides orogens is known as the Vardar zone (Arsovski, 1997; Dumurdzanov et al., 2005; Kossmat, 1924).

These structures are overprinted by Cenozoic extension, as part of the South Balkan extensional regime, a northern segment of the Aegean extensional system (Burchfiel et al., 2008). Two periods of extension are identified, separated by a short period of compression. During the first extensional period, in the middle to late Eocene, extensional basins developed in relation to trench rollback along the northern Hellenic trench. This was followed by shortening in the late Oligocene to Early Miocene due to the arrival of the Kruja fragment on the Albanian subduction front. The second period of extension (middle Miocene to present) is related to the progressive rollback of the subducted slab at the northern Hellenic trench, resulting in the development of several types of basins (e.g., true grabens, tilted half-grabens and pull-apart basins along strike-slip faults; Dumurdzanov et al., 2004, 2005) dominated by NW-SE and E-W-trending faults. The latter are associated with the propagation of the North Anatolian fault in the Aegean Sea at ~6 Ma that partly decoupled the South Balkan extensional system in the north from the Aegean extensional system in the south (Burchfiel et al., 2008; Dumurdzanov

et al., 2005). The still active fault lines and zones are marked by scarps and offsets on Quaternary deposits in the basins, as well as by the locations of numerous earthquakes in recent times (Drogreška, 2018).

The Cenozoic evolution of North Macedonia was accompanied by extensive volcanism. The first period of volcanism took place in the eastern part mainly during the early Oligocene (Boev & Yanev, 2001) and was marked by the formation of large volcanic complexes with subduction-related geochemical characteristics. On the other hand, the second period occurred during Late Miocene—Pleistocene times (<10 Ma), when the volcanic activity within the region was focused in the Vardar zone and it is largely connected to the tectonic evolution of the South Balkan extensional system (Molnár et al., 2022; Yanev et al., 2008). During the latter phase, mainly small mafic volcanic centers with within-plate geochemical characteristics developed. Exception is the large Kožuf-Voras volcanic complex, located along the North Macedonia—Greece border, which has subduction-related characteristics (Kolios et al., 1980; Molnár et al., 2022; Yanev et al., 2008).

North Macedonia, especially in its central part, shows a relatively shallow depth of the Moho with values comprising between 32 and 35 km along the Vardar suture (Boykova, 1999; Grigoriadis et al., 2016) connecting two regional minima of about 30 km depth, one in the south (North Aegean Sea) and one in the north (along the Danube close to Belgrade). The depth of the Moho steeply increases in the eastern direction reaching 50 km behind the border of Bulgaria. A smoother increase is observed toward the west, reaching depths that exceed 40 km in Albania (Boykova, 1999).

3. Materials and Methods

During 2019–2022, 65 samples of free and dissolved gases were collected throughout North Macedonia. Among them, 45 were sampled from cold to lukewarm manifestations (<28°C) and 20 from thermal discharges (28°C to >74°C) (Figure 1; Supporting Information S1 and Supporting Information S2). The list of the sampling locations is reported in Supplementary Information (Figure S1 and Table S1 in Supporting Information S1). Analyses of chemical and isotopic composition of gas samples were carried out at the laboratories of Istituto Nazionale di Geofisica e Vulcanologia of Palermo (INGV-Pa).

The data set produced for this study is integrated with literature data of gas emissions from Greece, Serbia, Albania, Kosovo and Bulgaria for regional scale discussion (Daskalopoulou et al., 2019; Lévy et al., 2023; Minissale et al., 2023; Piperov et al., 1994; Randazzo et al., 2021).

3.1. Field Sampling and Chemical Analysis

Bubbling gases were sampled using an inverted funnel positioned above the emission point of the highest flux, whereas soil gases were collected by inserting a pipe in the soil at >50 cm depth and driving the gas by a syringe and a 3-way valve. Dry gases were collected in glass flasks equipped with two stopcocks (20–150 ml of volume) and/or in Exetainer® Labco vials (12 ml). Samples for dissolved gas analyses were collected in glass bottles (150 ml) sealed underwater by gastight rubber/teflon plugs.

Chemical composition (He, H_2, H_2S, O_2, N_2, CO_2, and CH_4) of dissolved and free gas samples were analyzed by an Agilent 7890B gas chromatograph combined with a Micro GC analyzer by Inficon. Concentrations of CO_2 and H_2S were determined by the Micro GC analyzer with He as carrier and equipped with a Poraplot-U column and TCD detector (detection limit about 100 and 10 μmol mol^{-1}, respectively). All the other gases were determined by the GC system with Ar as carrier and equipped with a 4-m Carbosieve S II column. A TCD detector was used to measure the concentrations of He, H_2, O_2, N_2 (detection limit about 3, 2, 50, and 100 μmol mol^{-1}, respectively) and an FID detector for CH_4 (detection limit about 1 μmol mol^{-1}). The analytical errors were less than 10% for He, H_2, and H_2S, and less than 5% for the remaining gases.

Gases in the dissolved phase were analyzed following the "headspace technique" (Capasso & Inguaggiato, 1998) and were extracted after equilibrium was reached at a constant temperature with a host-gas (high-purity Ar) being injected in the sample bottle. The chemical composition of the dissolved gas phase was obtained from the gas-chromatographic analyses considering the solubility coefficients (Bunsen coefficient "β," ccgas L_{water}^{-1} STP) of each gas species, the volume of gas extracted and the volume of the water sample (Capasso & Inguaggiato, 1998; Liotta & Martelli, 2012). Starting from the total amount of dissolved gases (ccSTP L^{-1}), the relative abundances of each gas species in equilibrium with the dissolved gas phase were recalculated and the analytical

results were expressed in μmol mol^{-1} of gas at atmospheric pressure, allowing the comparison of gases found in dissolved and free phases.

3.2. Isotopic Analysis of C, He, and Ar

The $^{13}C/^{12}C$ ratios of CO_2 (expressed as $\delta^{13}C\text{-}CO_2$ ‰ vs. V-PDB) were measured with a Finnigan Delta S mass spectrometer after purification of the gas mixture by standard procedures using cryogenic traps (precision $\pm 1\sigma = 0.1$‰).

Helium isotope composition was analyzed directly from the sample bottles after purification in the high-vacuum inlet line of the mass spectrometer. The isotope composition of dissolved He was analyzed by headspace equilibration (Inguaggiato & Rizzo, 2004; Italiano et al., 2014). The $^3He/^4He$ and $^4He/^{20}Ne$ ratios were determined after cryogenic separation by a GVI Helix SFT mass spectrometer. The analytical errors were, generally, <1%. Helium isotope composition is expressed as R/R_A, namely $^3He/^4He$ of the sample versus the atmospheric $^3He/^4He$ ($R_A = 1.386 \times 10^{-6}$; Ozima & Podosek, 2002).

Argon concentration and its isotope composition (^{40}Ar, ^{38}Ar and ^{36}Ar) were analyzed by mass spectrometry, using a multi-collector Helix MC-GVI, with analytical uncertainty (1σ) for single $^{40}Ar/^{36}Ar$ measurements of <0.05%.

4. Results

4.1. Chemical Composition of the Gases

The chemical composition (He, H_2, H_2S, O_2, N_2, CO_2, CH_4, and Ar) of the collected samples, together with the isotopic composition of C in CO_2, He and Ar, as well as their coordinates and the physico-chemical parameters of related waters are included in an open-access data set (Li Vigni et al., 2025).

Nitrogen and CO_2 are the most abundant gas components with concentrations that range from 1,300 to 989,200 μmol mol^{-1} and from 112 to 999,000 μmol mol^{-1}, respectively. Ar and O_2 show concentrations up to 11,100 μmol mol^{-1} and 205,700 μmol mol^{-1}, respectively. Methane concentration varies from 2 to 7,100 μmol mol^{-1}. Only the samples collected at Smokvica (Figure S1 and Table S1 in Supporting Information S1) present a slight enrichment in CH_4 with values up to 22,500 μmol mol^{-1}. Hydrogen sulfide varies from <10 to 12,800 μmol mol^{-1}. Helium values are up to 3,600 μmol mol^{-1}.

Based on the measured gas composition, the data set has been divided into three groups: (a) N_2-dominated (N_2 from 822,800 to 989,200 μmol mol^{-1}), (b) CO_2-dominated (CO_2 from 474,200 to 999,000 μmol mol^{-1}), and (c) H_2S-rich (H_2S from 11 to 12,800 μmol mol^{-1}) (Figure 2). The 3rd group consisted of N_2- and CO_2-dominated gases that presented H_2S enrichments up to 1%. From this group, the N_2-dominated gases correspond to gas that are found in the dissolved gas phase, whilst the CO_2-dominated gases include only free gas samples. It is worth noting that even though the dissolved gas samples of Botun 1 and Kiselo Klajnče do not have H_2S in their gas composition, they are also included in this group. These samples are located in the vicinity of Botun and Petkoniva (Figure S1 and Table S1 in Supporting Information S1) that show enhanced H_2S contents but, as will be discussed in Section 5.3, their inclusion was not based only on geographical criteria.

4.2. Isotopic Composition of the Gases

The $\delta^{13}C\text{-}CO_2$ values vary between −15.7 and + 1.0‰. The N_2-dominated gases show the most negative $\delta^{13}C\text{-}CO_2$ values (from −15.7 to −3.2‰). Most CO_2-dominated and H_2S-rich gases show $\delta^{13}C\text{-}CO_2$ values from −4.6 to +1.0‰ and from −1.7 to +0.70‰, respectively. Few samples belonging to the CO_2-dominated group (Geogas, Kozica 1 and Krušeani. Figure S1 and Table S1 in Supporting Information S1) show $\delta^{13}C\text{-}CO_2$ values from −7.7 to −6.5‰.

The isotopic composition of He varies from 0.1 to 1.8 R_A with $^4He/^{20}Ne$ ratios ranging between 0.5 and 2066. Samples of the N_2-dominated group have R/R_A and $^4He/^{20}Ne$ ranging from 0.15 to 1.09 and from 1.25 to 203, respectively. Gases of the CO_2-dominated group show R/R_A values between 0.1 and 1.8, with corresponding $^4He/^{20}Ne$ ratios from 0.5 to 473. The H_2S-rich group shows R/R_A between 0.08 and 0.36, whereas $^4He/^{20}Ne$ ratios range between 11.2 and 2066.

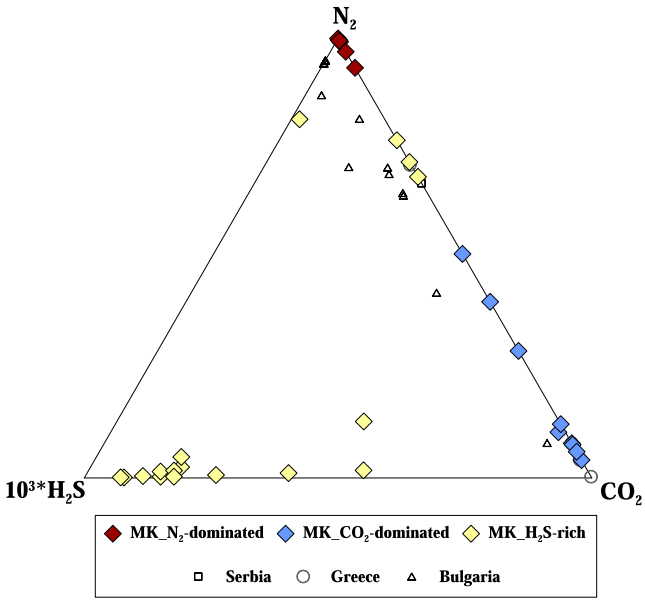

Figure 2. Chemical composition of the sampled gases. H_2S-CO_2-N_2 ternary diagram. Data from the neighboring countries are included: Bulgaria (Minissale et al., 2023; Piperov et al., 1994), Greece (Daskalopoulou et al., 2019), and Serbia (Randazzo et al., 2021).

The N_2-dominated group shows isotopic compositions of argon comprising between 294 and 302 for $^{40}Ar/^{36}Ar$ and between 0.187 and 0.191 for $^{38}Ar/^{36}Ar$. The $^{40}Ar/^{36}Ar$ of CO_2-dominated samples ranges between 285 and 307, with corresponding $^{38}Ar/^{36}Ar$ in the range of 0.182–0.198, while the gases of H_2S-rich group show $^{40}Ar/^{36}Ar$ values that vary from 295 to 372 and $^{38}Ar/^{36}Ar$ ratios that range between 0.186 and 0.191 (Figure S2 in Supporting Information S1).

5. Discussion

The three identified groups of gases (N_2-dominated, CO_2-dominated and H_2S-rich gases) are geographically moderately well separated (Figure 3). The manifestations characterized by N_2-dominated gases are located in the easternmost part of the country and comprise the geothermal fields of Kežovica, Gevgelija, and Strumica, as well as the Dobra borehole of the Kočani geothermal field, and the cold gas manifestation of Rakliš. The CO_2-dominated group is mostly located in the central part of the country and includes gas samples from the thermal springs of Kumanovo and Katlanovo, from the geothermal fields of Kumanovo and Skopje, the Istibanja borehole in the Kočani geothermal field, and almost all of the cold gas manifestations: (a) Smrdliva Voda, Gorničet, Makedonka Češma, and Topli Dol in the mountainous border of Kožuf Mts. west of the Gevgelija basin; (b) Lešok and Banjiče, near the Polog basin; (c) Pelagonia basin, in south-west of the country. Lastly, all the gas samples of the H_2S-rich group are located in a narrow area within the Debar geothermal field, Botun and Kosel, in the

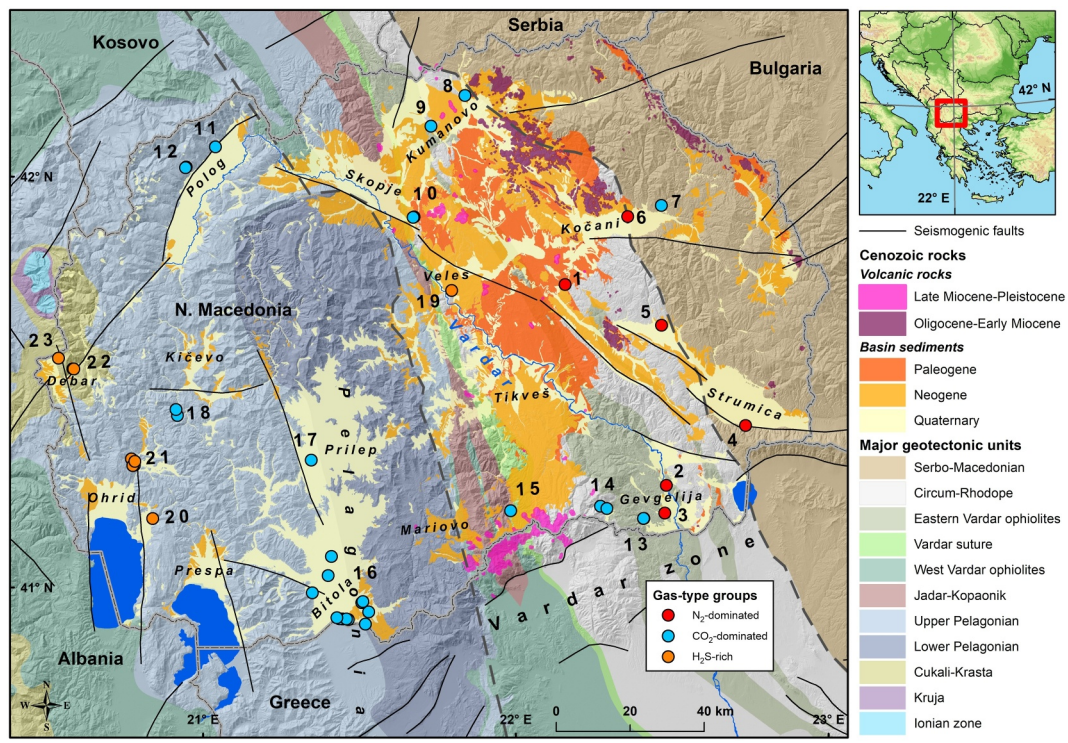

Figure 3. Spatial distribution of the three identified gas-type groups. Sampling sites as in Figure 1. Main geotectonic units from Schmid et al. (2020). Extension of Cenozoic sediments after Dumurdzanov et al. (2004, 2005) and volcanic rocks after Molnár et al. (2022). Seismogenic crustal faults from the European Database of Seismogenic Faults (EDSF; https://edsf13.ingv.it/). Dashed black lines approximate the extent of the Vardar zone. Extensional basins and geothermal fields mentioned in the text are also indicated.

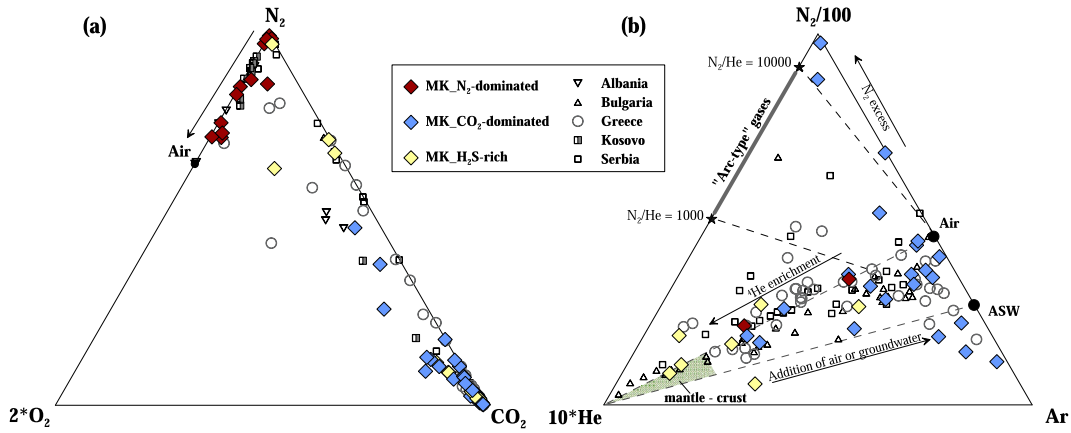

Figure 4. (a) O_2-CO_2-N_2 and (b) He-Ar-N_2 ternary diagrams. The atmospheric air (N_2/Ar = 83—Giggenbach et al., 1983), Air Saturated Water (ASW; N_2/Ar = 38—Fischer et al., 1998), arc-type, mantle and crustal gases (Giggenbach, 1996) compositions are also plotted. Data from the neighboring countries are included: Albania (Lévy et al., 2023), Bulgaria (Minissale et al., 2023; Piperov et al., 1994), Greece (Daskalopoulou et al., 2019), Kosovo (Lévy et al., 2023), and Serbia (Randazzo et al., 2021).

westernmost part of the country, with the only exception being the Sabotna Voda that is close to Veles town (Figure 3).

5.1. Origin(s) of N_2 and Ar

Samples collected from North Macedonia present N_2/O_2 ratios mostly higher than air (Figure 4a). This is indicative of inorganic or/and organic redox reactions that take place in the subsoil or in the aquifer consuming O_2, virtually enriching N_2 in the samples that present concentrations up to 989,200 μmol mol^{-1}. These processes mostly affect dissolved gas samples. If no additional gases mix in while the water circulates through the aquifer, the dissolved gases that are already depleted in O_2 will not generate enough pressure to form a separate free gas phase. Therefore, the atmospheric component will remain dissolved until the water reaches the spring outlet. As a result, N_2-dominant gases are most commonly found in dissolved gas samples. Notable exceptions are the gases from the thermal springs of Negorci, Smokvica, and Bansko (Figures 1 and 3), where the N_2 solubility is lowered by the high temperatures (45–74°C) of the waters, leading to the separation of a N_2-rich free gas phase. Addition of non-atmospheric N_2 may also be a possibility. However, in the absence of N_2 isotopic data, this hypothesis cannot be confirmed.

Samples from Bansko, Dobra, Kežovica, and Rakliš deviate from the N_2-CO_2 alignment toward the compositional point of atmospheric air (Figure 4a). The presence of abundant O_2 (up to 157,800 μmol mol^{-1}) together with the N_2/O_2 ratios show values close to the atmospheric one, thereby suggesting a possible shallow atmospheric input. In the case of soil gases, such components may mostly derive from atmospheric air diffusion within the soil. In the case of bubbling gases, the mixing with a shallow aquifer in equilibrium with the atmosphere should be considered as well. In both cases, some contamination during sampling cannot be ruled out.

The He-Ar-N_2 ternary diagram (Figure 4b) is a helpful tool to discriminate mixing processes between crustal, mantle, and atmospheric components (Giggenbach et al., 1983). The majority of the samples are found inside the triangle delimited by the He apex and N_2/Ar of air saturated waters (ASW) and air (N_2/Ar = 83.6 and 36.9 at 20°C, respectively, Kipfer et al., 2002). This distribution suggests a two-component mixing relationship between geogenic (crustal or magmatic) and atmospheric sources. The deep component is more evident in the H_2S-rich category, likely due to a long residence time in the crust (Mazor, 1991). Most of the CO_2-dominated samples show N_2/Ar ratio values close to either atmospheric or air-saturated water points. This suggests that N_2 and Ar of prevailing atmospheric origin are added to the uprising gases by the meteoric recharge of the hydrologic circuit that is feeding the sampled manifestations. Nevertheless, the atmospheric origin is supported by the isotopic composition of Ar (^{36}Ar, ^{38}Ar, and ^{40}Ar). The atmospheric mixture is composed mainly of ^{40}Ar, but the ^{36}Ar is considered exclusively of atmospheric origin, whilst the ^{40}Ar budget derives from the radiogenic decay of ^{40}K in the crust (Holland & Gilfillan, 2013). The gas samples have a small range of Ar isotopic values, mostly close to

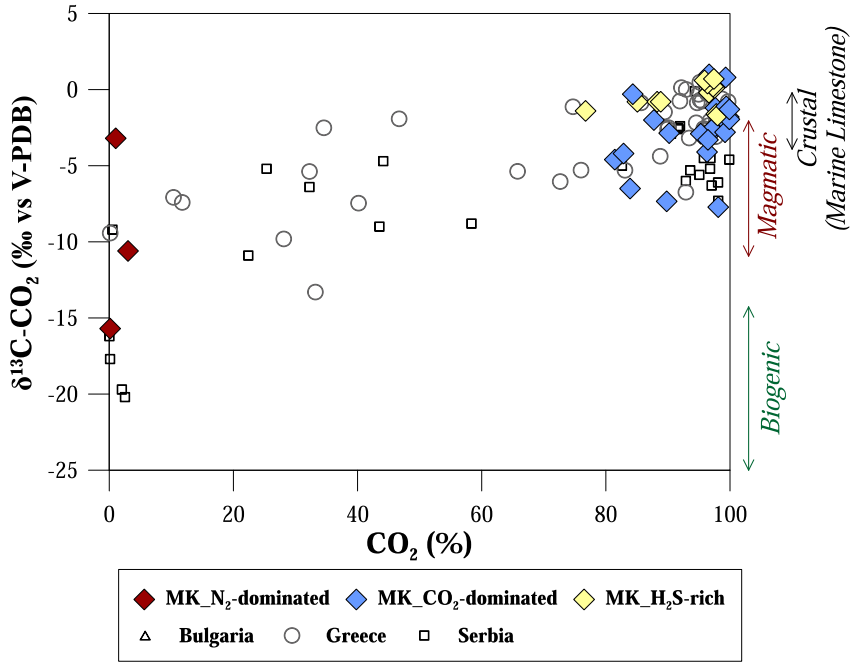

Figure 5. Binary plot of CO_2 concentrations (%) versus $\delta^{13}C$-CO_2 (‰ vs. V-PDB) values. The three, colored arrows represent the $\delta^{13}C$-CO_2 ranges of the three different sources (from Jenden et al., 1993): biogenic (green), magmatic (red), and crustal (black). Data from the neighboring countries are included: Bulgaria (Minissale et al., 2023; Piperov et al., 1994), Greece (Daskalopoulou et al., 2019) and Serbia (Randazzo et al., 2021).

the typical atmospheric signature ($^{40}Ar/^{36}Ar$ = 298.56 and $^{38}Ar/^{36}Ar$ = 0.188; Lee et al., 2006; Ozima & Podosek, 2002). Exceptions are the samples from Busemak, Geogas, Pela Rosa and Kozica 1, all in the Bitola basin, that present a high N_2/Ar ratio (from 134 to 5,383; Figure 4b), pointing toward a possible addition of non-atmospheric N_2 (metamorphic and/or from decay of organic matter; Haendel et al., 1986; Javoy et al., 1984; Jenden et al., 1988).

5.2. Source(s) of CO_2 and He

Carbon dioxide is one of the major deep gases and represents the main carrier of mantle-derived fluids. The $\delta^{13}C$-CO_2 versus CO_2 diagram (Figure 5) allows discrimination between the diverse possible carbon sources: biogenic, magmatic, and crustal. The results show that the gas samples fall mostly within the typical range for crustal and magmatic carbon (Figure 5). Exception is the Smokvica sample that presents the lowest isotopic carbon value (−15.7‰), because of isotopic fractionation, likely, due to a strong CO_2 loss (Figure S4 in Supporting Information S1).

Considering a mixing model between magmatic carbon and crustal, both reduced and oxidized, carbon (Figure S3 in Supporting Information S1), a possible crustal contribution may be derived from decarbonation processes within carbonate rocks by means of a heat source (e.g., intrusion of a magmatic body into the crust), which forms metamorphic CO_2 with a mean value of $\delta^{13}C$ of about 0.3‰ (Clark & Fritz, 1997; Hunt, 1996). Any contributions from organic sediments to fluids deriving from a descending slab are limited. Nonetheless, the isotopic signature of metamorphic CO_2 is a topic of ongoing debate; some authors have reported ^{13}C values of the CO_2 similar to those of source rocks (e.g., Sharp et al., 2003), whilst others have observed that metamorphic decarbonation processes produce CO_2 fluids enriched in ^{13}C up to +3.8‰ compared to the carbon of the protoliths (e.g., Evans et al., 2008; Marini & Chiodini, 1994).

Metamorphic decarbonation reactions occur commonly during regional metamorphic processes and involve carbonate-bearing metasediments. These reactions are triggered by increasing temperature and pressure, resulting in the reaction of carbonate minerals with silicate minerals that results in the formation of Ca-silicate minerals and the release of CO_2 (Stewart et al., 2019). This applies to the thermal samples from Istibanja, Katlanovo and

Kumanovo hydro-systems, whose reservoirs are hosted in carbonate-rich aquifers (Precambrian gneiss and Paleozoic carbonate schist, Precambrian and Paleozoic marbles, and Paleozoic marbles, respectively; Popovska-Vasilevska & Armenski, 2016). In these samples, decarbonation reactions are favored by high temperatures (Gorgieva, 1989). Another possibility is that metamorphic decarbonation reactions occur in fault core zones (Kleine et al., 2014), where CO_2-bearing fluids and rocks are in disequilibrium. The flow of fluids within the rocks surrounding the fault structure remains slow in comparison to the decarbonation reaction rate, thereby buffering the fraction of CO_2 contained within this fluid. Conversely, fluid channeled along the fault core zone shows higher flux compared to the surrounding rocks, inhibiting the progress of decarbonation reactions (Kleine et al., 2014).

Because of the multiple carbon sources (e.g., hydrocarbon oxidation, organic matter decay, respiration, decarbonation of marine carbonates and degassing of magmatic bodies) and the numerous secondary, deep or shallow processes (e.g., fluid-rock interactions, dissolution, mixing, redox reactions) that may isotopically fractionate CO_2 (Jenden et al., 1993; Wycherley et al., 1999), the interpretation of $\delta^{13}C$-CO_2 values alone does not provide direct evidence to the origin of the fluids (note the overlapping magmatic and crustal fields around −4‰ in Figure 5). The isotope composition of noble gases (He, Ne, and Ar) and the comparison with the carbon isotope composition are more effective to distinguish the fluid origin and quantify possible mixing between the different sources; inert noble gases have a more distinct isotopic signature in terrestrial reservoirs (atmosphere, mantle, and crust; Holland & Gilfillan, 2013).

The coupled R/R_A and $^4He/^{20}Ne$ ratios (Figure 6a) can be used to identify and quantify the possible sources of He. Gas samples belonging to the CO_2- and N_2-dominated groups show a prevailing crustal source of He (continental crust 0.01–0.02R_A; Ballentine & Burnard, 2002), with a mantle contribution between 1% and 20%, considering a Mid Ocean Ridge (MOR) end-member (R/R_A 8 ± 1; Ozima & Podosek, 2002). As North Macedonia is located in a continental setting subjected to an extensional tectonic regime, the European Subcontinental Lithospheric Mantle (ESCLM, with R/R_A value of 6.32 ± 0.39; Gautheron et al., 2005) could be considered as an alternative mantle end-member to MOR (Figure 6a). For instance, assuming the ESCLM, mantle contribution arrives at 25% for the samples with the highest R/R_A ratios (Figure S4 in Supporting Information S1). Li Vigni et al. (2022) and Molnár et al. (2021) suggested that the mantle source beneath the study area could be characterized by an even more radiogenic value for He, as geochemical characteristics of the youngest volcanic rocks suggest the occurrence of a metasomatized lithospheric mantle in the area (Molnár et al., 2022; Yanev et al., 2008). This is also supported by the lower R/R_A values than the ESCLM (between 3.1 and 4.5) that were obtained from fluid inclusions in olivine phenocrysts hosted in the Pleistocene (1.8 ± 0.1 Ma) lavas of Mlado Nagoričane volcanic center in Kumanovo basin (Molnár et al., 2021). If the mantle beneath North Macedonia is indeed contaminated by subduction-related U-Th-rich crustal material, then the mantle contribution will potentially exceed 25%.

The highest mantle input in the studied samples was found in two areas. The first is recognized in the southern part of the country, along the Nidže-Kožuf mountains, between Mariovo and Gevgelija grabens. This may be related to the activity of the Neogene-Quaternary Kožuf-Voras volcanic system (Kolios et al., 1980; Molnár et al., 2022, 2023). Studies on hypogene karst systems of this area indicate fluid circulation along deep fault systems causing groundwater interaction with the rocks of the Kožuf-Voras volcanic system and consequently the addition of metamorphic CO_2 and up to 10% mantle He to the water (Temovski et al., 2021, 2022). The second area with high mantle input for He is found in the northern part of the country, on the western side of the Polog graben close to Tetovo. Here, enhanced $^3He/^4He$ ratios may be associated with an active regional fault system and/or with the seismically active secondary normal faults found in the border of the basin (Dumurdzanov et al., 2005). Such faults may act as preferential escape pathways for mantle fluids.

With regard to the crustal source of He, one potential origin is attributable to the radiogenic decay of U and Th from granitic intrusions and metamorphic rocks within the crust, which increase the ^4He concentration in the circulating fluids. This process may occur in geothermal fields located in the eastern part of the country, within the Serbo-Macedonian Zone, where Precambrian crystalline basement and granitic intrusions are present. As previously mentioned, gas samples collected from these geothermal systems are N_2-dominated, have low R/R_A ratios (<1.1), and show a high He content (up to 3,600 μmol mol^{-1}). Interestingly, the reservoirs of these systems are hosted in Paleozoic granite and/or Paleozoic metamorphic formations (Gorgieva et al., 2000; Micevski et al., 2007; Naunov, 2003; Spasovski, 2012), where radiogenic decay can produce significant amounts of ^4He.

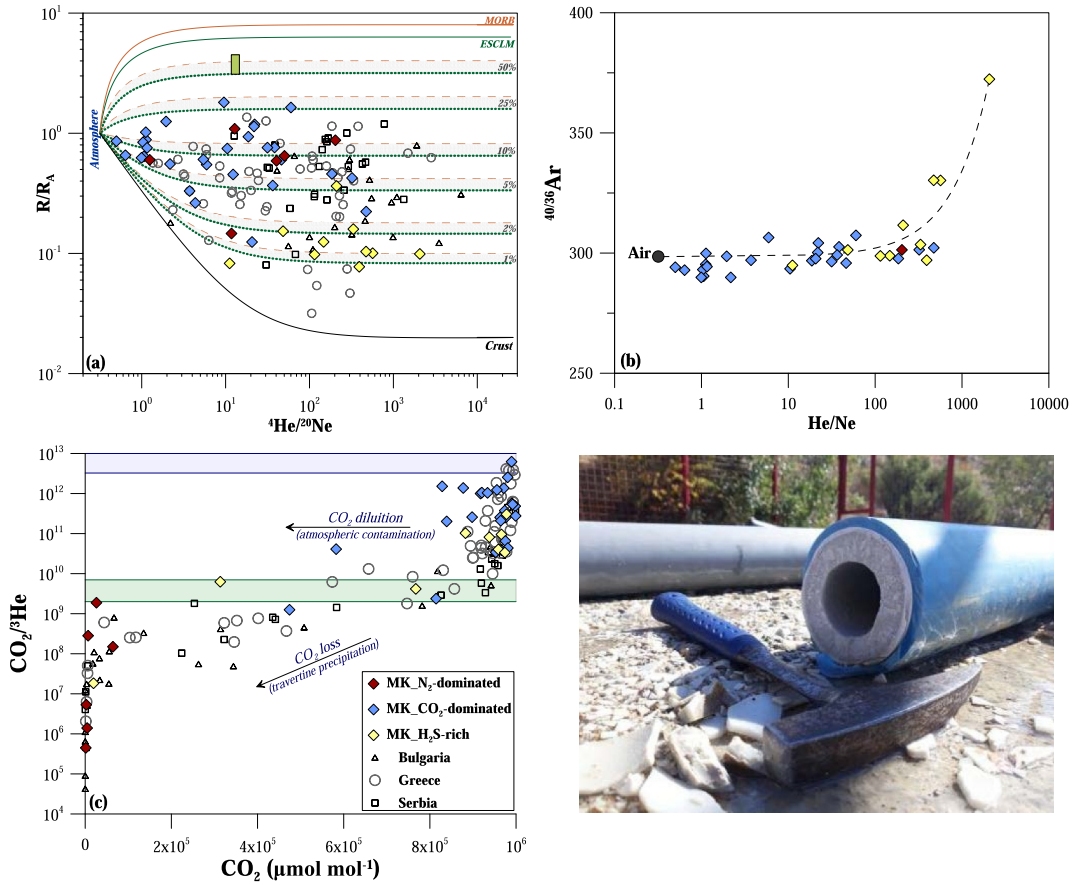

Figure 6. (a) Binary plot of R/R_A ratio versus $^4He/^{20}Ne$ ratio. The dashed lines represent the mixing between atmosphere ($1R_A$, Ozima & Podosek, 2002; $^4He/^{20}Ne = 0.318$, Sano & Wakita, 1985), crust (0.01–0.02R_A, Ballentine & Burnard, 2002; $^4He/^{20}Ne > 1{,}000$, Sano & Wakita, 1985), MORB-type (8 ± 1 R_A, Ozima & Podosek, 2002; $^4He/^{20}Ne > 1{,}000$, Sano & Wakita, 1985) and ESCL-type (6.32 ± 0.39 R_A, Gautheron et al., 2005; $^4He/^{20}Ne > 1{,}000$, Sano & Wakita, 1985) mantle at different percentages. The green area represents the R/R_A and $^4He/^{20}Ne$ data from fluid inclusions hosted in olivine phenocrystals from the Mlado Nagoricăne volcanic center (North Macedonia) (Molnár et al., 2021). (b) Binary plot of $^{40}Ar/^{36}Ar$ ratio versus $^4He/^{20}Ne$ ratio. The dashed lines represent the mixing between the atmosphere ($^{40}Ar/^{36}Ar = 298.56$; Lee et al., 2006; $^4He/^{20}Ne = 0.318$, Sano & Wakita, 1985) and the Macedonian sample with the highest argon ratio. (c) Binary plot of CO_2 concentration (µmol mol^{-1}) versus $CO_2/^3He$ ratio. The shaded regions highlighted the $CO_2/^3He$ values of ESCLM ($CO_2/^3He$ from 2 to 7×10^9; Bräuer et al., 2016; Marty et al., 2020) in green, and the crust in blue. (d) Picture of calcite deposition in a pipe at the Katlanovo sampling site.

Some samples, mostly from the CO_2-dominated group, are characterized by $^4He/^{20}Ne$ ratios that are close to the atmospheric end-member (0.318, Sano & Wakita, 1985). This indicates a strong atmospheric input likely related to the composition of the gas dissolved in the waters through which they bubble or due to mixing between the deep-circulating fluids and shallower air-saturated waters. On the contrary, the atmospheric contribution is negligible for the gas samples of the H_2S-rich ($^4He/^{20}Ne$ ratios >11). These samples present low R/R_A values (all except one from 0.08 to 0.16), indicating a nearly pure crustal origin for He ($R/R_A < 0.16$ R/R_A correspond to <2% of mantle contribution—Figure 6a). A negligible non-atmospheric contribution to these gases can also be highlighted by the isotope composition of Ar (Figure 6b). Gas samples from Botun, and Kosel seem to have experienced minor ingrowths of ^{40}Ar (up to $^{40}Ar/^{36}Ar = 372$; Figure 6b). Considering the positive correlation of the $^{40}Ar/^{36}Ar$ ratios with the $^4He/^{20}Ne$ ratios and the corresponding crustal-derived $^3He/^4He$ ratios of the former, an additional crustal input from radioactive decay of ^{40}K cannot be excluded.

The sample of Sabotna Voda, which is the only H_2S-rich sample located outside the westernmost area, displays a mantle contribution of nearly 5% (R/R_A 0.36). This contribution is much higher with respect to the remaining samples of this group. The ultrapotassic mafic volcanic center of Kišino, the youngest volcanic site in Macedonia

(1.5 Ma—Yanev et al., 2008) that is found nearby, east of Sabotna Voda, possibly justifies the small mantle He contribution in this spring.

The combination of CO_2 and ^3He, expressed as $CO_2/^3He$ ratio, is used to evaluate any depletion or enrichment relative to the mantle signature of the fluid. Figure 6c compares the $CO_2/^3He$ ratio with the CO_2 concentration of the collected gases. The $CO_2/^3He$ values of the studied gas samples varied between 4.5×10^5 and 6.2×10^{12}, showing a wide range spanning over seven orders of magnitude. The collected gas samples of the CO_2-dominated and H_2S-rich groups mostly have higher $CO_2/^3He$ ratios (1.2×10^9–6.2×10^{12} and 1.8×10^7–3.1×10^{11}, respectively) and are distributed in the area found between the crust and ESCLM ranges. Samples that plot above the ESCLM range demonstrate very low ^3He concentrations, indicating a prevailing crustal source of CO_2 due to geogenic (i.e., metamorphic decarbonation reactions; Figure 5) or biogenic processes (Sano & Marty, 1995). Conversely, samples that plot within or close to the ESCLM range have a significant amount of ^3He. This suggests either a prevailing mantle contribution or a loss of CO_2 during gas-water-rock interactions. Gases of the N_2-dominated group and Sabotna Voda (H_2S-rich group) present low $CO_2/^3He$ ratios. Considering their chemical and isotopic compositions, the occurrence of secondary processes that changed the pristine composition of the gases is possible. One explanation for the CO_2 loss is the deposition of thermogenic travertine (mineral trapping), a common secondary process occurring within geothermal systems (Barry et al., 2020; Gilfillan et al., 2009; Ray et al., 2009; Stefánsson et al., 2017). The solubility of CO_2 in water depends on the temperature and pressure conditions of the water; high temperature results in a decreased CO_2 solubility. The dissolution of large quantities of CO_2 may result in chemical disequilibria within the aquifer, potentially leading to reactions that involve the dissolution and precipitation of minerals (Baines & Worden, 2004). On dissolution in circumneutral to alkaline groundwater, CO_2 reacts with H_2O and forms H_2CO_3. The latter rapidly dissociates into HCO_3^- and CO_3^{2-} ions and reacts with Ca^{2+} and Mg^{2+} ions. Extensive CO_2 dissolution in the hydrothermal environment may result in the oversaturation of calcite and/or aragonite, leading to the precipitation of these mineral phases (Stefánsson et al., 2016, 2017). This causes a strong decrease of CO_2 content, with a consequent virtually increase of N_2 concentration, and a fractionation of $\delta^{13}C$ values, thus increasing the lighter component in the residual gases. The pH range, which spans from 6.9 to 8.8, the high temperature (up to 70°C), and the extensive travertine deposition located in these geothermal systems supports this hypothesis (Figure 6d). Randazzo et al. (2021), following the model proposed by Gilfillan et al. (2009), interpret the presence of N_2-dominated manifestation in Serbia as the result of varying degrees of CO_2 loss by dissolution processes occurring at pH values between 5.6 and 7. This leads to an enrichment of the fluids in N_2. No travertine deposits are found near Sabotna Voda, where the CO_2 loss is likely due to a differential dissolution caused by the interaction with shallow aquifers during its migration toward the surface (Ray et al., 2009). In this case, the higher solubility of CO_2 (solubility trapping) with respect to N_2 and noble gases in aquatic systems results in the enrichment of the latter gas species (Ozima & Podosek, 2002; Figure 6c).

5.3. Origin of H_2S

Hydrogen sulfide in natural gases can be found in three main geogenic environments: magmatic (e.g., Allard et al., 1991; Giggenbach, 1987), hydrothermal (Giggenbach, 1997; Ohmoto & Lasaga, 1982), and sedimentary systems. Among the latter, the main H_2S generating processes are the alteration of sulfide minerals (e.g., Giggenbach, 1980), the reactions of sulfate reduction (e.g., Machel, 2001), and the emission from shallow sediments rich in organic matter and anoxic waters (Thode, 1991).

The presence of H_2S in the fluid can be related to the evaporitic sulfate minerals that are found in the stratigraphic sequences of the area. Evaporite outcrops of supposedly Upper Cretaceous age (gypsum, anhydrides, salts, multicolored clays and breccias with interbedded dolomite and thin organic-rich shales) are present in the western part, on Dešat and Stogovo mountains near Debar (Frashëri et al., 1996; Jančev et al., 1999), whilst Triassic evaporite (Ionian unit; Schmid et al., 2020) is only hypothesized at depth in Duvalo Kosel, Botun and Petkoniva areas (Li Vigni et al., 2022).

Hydrogen sulfide might be produced during either thermochemically (TSR) or microbially (MSR) driven sulfate reduction processes (Machel, 2001) that occur in these evaporite deposits. TSR processes take place in deep burial settings in a temperature range between 100°C and 140°C (Machel, 2001), such as in gas provinces of western Canada (Manzano et al., 1997), the United States (Heydari, 1997) and Abu Dhabi (Worden et al., 1996). On the other hand, MSR is widespread in shallow burial environments in a temperature range of 0–80°C (Machel, 2001).

The latter process was observed in the Frasassi cave system (northeastern Apennines, Italy), where several H_2S-rich springs are present. In this case, the H_2S is produced through bacterial sulfate reduction in black shale within deep-seated Triassic evaporites (D'Angeli et al., 2019; Peterson et al., 2013).

At the Duvalo site, the most extended H_2S-rich gas manifestation of the area, the gas derives from thermochemical sulfate reduction (Li Vigni et al., 2022). According to the authors, this hypothesis is further supported by the isotopic composition of methane, which suggests a thermogenic origin, and the tectonic contact between sulfate-bearing strata and organic-rich shales of metamorphic basement, which favor sulfate reduction reactions. However, for the other sites, the contribution of microbially mediated sulfate reduction cannot be excluded. Data on the isotopic composition of sulfur are currently not available.

Gas samples of Botun and Kiselo Klajnče were included in the group of H_2S-rich gases. Even though H_2S is below the detection limit in these gases, they are included in group iii due to their geographical position. Specifically, they are found in the area of Botun, close to Duvalo. There, free gas samples showed a CO_2-dominated composition while the dissolved ones were N_2-dominated. The endogenous gases on their transit toward the soil surface interact with a series of shallow cold aquifers or with stagnant meteoric water accumulations at the surface. Consequently, H_2S can dissolve in water due to its higher solubility with respect to other main gases. The high solubility may also justify the lower CO_2 content compared to the nearby free gas samples. As the solubility increases according to $N_2 < CO_2 < H_2S$, the generation of a gas with H_2S below the detection limit and with N_2 as the prevailing gas species is plausible. Furthermore, the disappearance of H_2S can be attributed to biologically and/or inorganically driven oxidation processes within the soil (Wróblewski et al., 2024). Oxidation reaction produces great quantities of H^+ ions, which increases the ionic power and acidifies the water. This explains the low pH values (4.5–5.5) of the water measured at the sampling points, which cannot be justified only by the amount of dissolved CO_2.

For Sabotna Voda, collected in the central part of the Vardar zone, although Triassic rocks are present nearby, no evaporite formations have been identified in the sequence (Arsovski, 1997). Thus, the presence of H_2S might derive from reduction processes of sulfate coming from either Triassic limestone-bound sulfate or may be related to S-rich coal beds within the Veles basin (Dumurdzanov et al., 2004).

6. Tectonic Implications

Data from the gas manifestations of North Macedonia are compared with those from the neighbor countries of Greece (Daskalopoulou et al., 2019), Serbia (Randazzo et al., 2021), Albania, Kosovo (Lévy et al., 2023), and Bulgaria (Minissale et al., 2023; Piperov et al., 1994). The gas manifestations of the South Balkan Peninsula are mainly related to the extensional tectonic structures of the area, with the impact of the latter being reflected in their spatial distribution (Figure 7). Such structures are associated with boundaries between the major geotectonic units, that is, the Vardar suture. The spatial distribution of the dominant gas follows a general trend from west to east (Figure 7a), with CH_4-dominated manifestations observed in Albania (west), CO_2-dominated ones in North Macedonia, and N_2-dominated ones in Bulgaria (east).

Albania is recognized as an oil and gas province, where several reservoirs are exploited (Nieuwland et al., 2001; Velaj, 2015). Several oil seeps and some reservoirs are also found in western Greece (Etiope et al., 2013; Zelilidis et al., 2015). The hydrocarbon fields are linked to the sedimentary regime, in which organic matter is abundant, favoring the occurrence of hydrocarbon deposits (Daskalopoulou et al., 2018). They belong to carbonate reservoirs of the Ionian fold-and-thrust belt and are related to the presence of Triassic evaporitic rocks, which provided an efficient seal for the oil and gas migration (Bega & Soto, 2017 and reference therein). Moreover, some CH_4-rich manifestations are associated to ophiolite complexes, such as the Mirdita ophiolite complex in Albania and Kosovo (Lévy et al., 2023; Truche et al., 2024), or the Pindos, Othrys, and Argolis ophiolite massifs in Greece, where abiotic CH_4 formation has been attributed to ongoing serpentinization processes (D'Alessandro et al., 2018; Etiope et al., 2013; Li Vigni et al., 2021).

Moving eastwards, CO_2-dominated gas manifestations became widespread in the region (Figures 7a and 7b). Two possible geogenic carbon sources are hypothesized for two different parts of the country. In the case of some geothermal fields, such as Istibanja, Katlanovo and Kumanovo hydro-systems in the eastern part of North Macedonia, CO_2 is associated with metamorphic decarbonation reactions within their reservoirs as they are hosted in carbonate rocks (Popovska-Vasilevska & Armenski, 2016). On the other hand, in the western part of

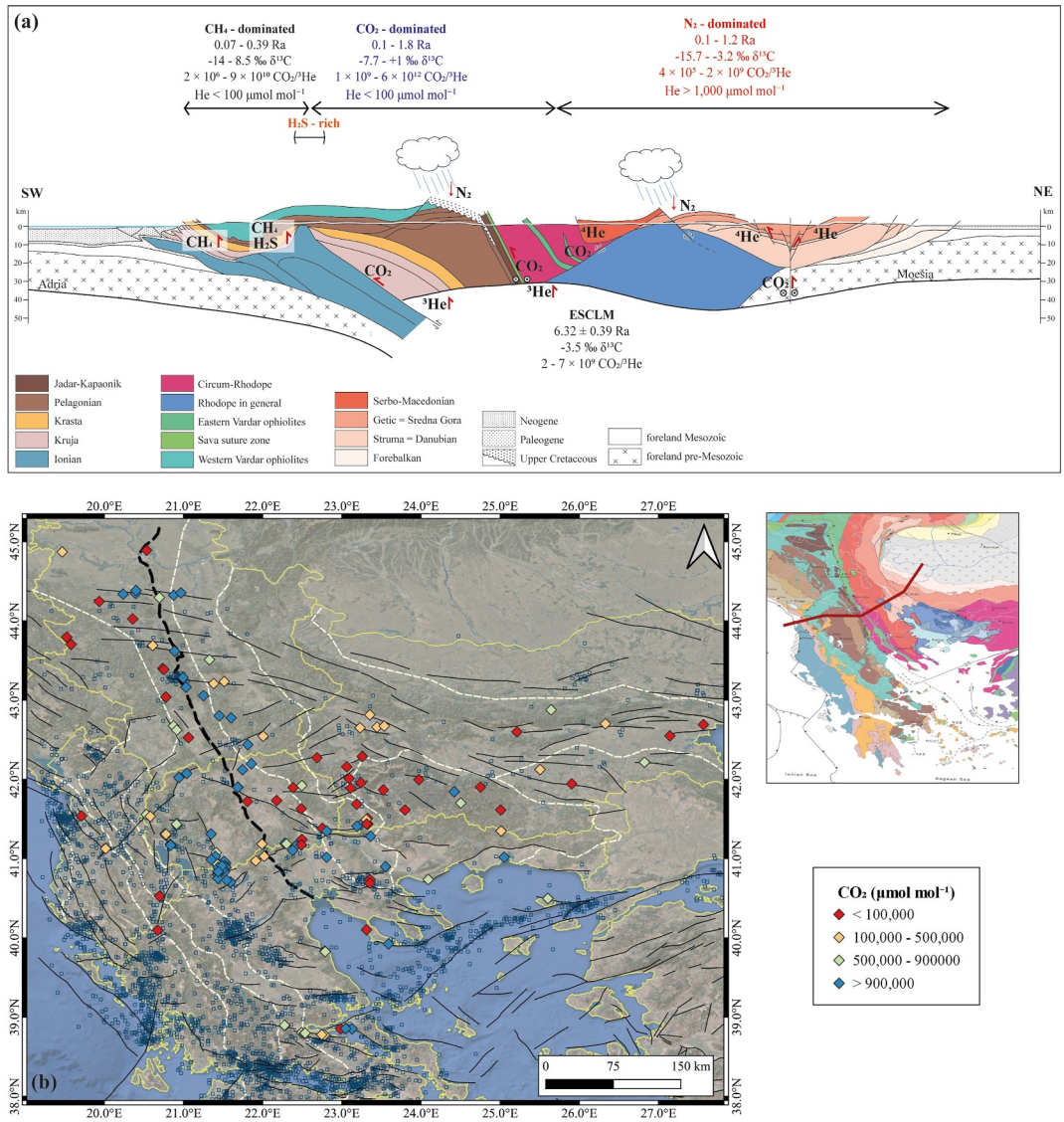

Figure 7. (a) Geological section from Schmid et al. (2020). Location of geological section is also added. Red arrows represent the potential fluid pathways. (b) Geographical distribution of CO_2 concentrations (µmol mol^{-1}) of the Southern Balkan Peninsula. Crustal faults (black lines) from the European Database of Seismogenic Faults (EDSF) compiled in the framework of the Project SHARE by INGV (https://edsf13.ingv.it). Earthquakes (blue squares) with a magnitude of ≧M4 and median depth value of 13 km, since 1960, from the USGS Earthquakes Hazard Program (https://earthquake.usgs.gov/earthquakes/search/). The black dashed line represents the Vardar suture, whilst the white dashed line represents the border of the geotectonic units. Data from this study: Daskalopoulou et al. (2019); Lévy et al. (2023); Minissale et al. (2023); Piperov et al. (1994); Randazzo et al. (2021).

North Macedonia, CO_2 of the cold CO_2-rich manifestations is linked to the active deep fault structures bordering Cenozoic horst-graben systems, where seismic activity is concentrated (Figure 7b; Burchfiel et al., 2008; Cvetkovic et al., 2016; Dumurdzanov et al., 2005) and favored also by the relatively shallow Moho in this area (Boykova, 1999). This points to a deeper origin of CO_2 (mantle or descending slab) in this area with respect to the eastern part. Historically, the western part of the Southern Balkan extensional regime has been affected by several moderate to strong earthquakes, and sometimes with destructive character, such as the M 6.1 in 1963 at Skopje (North Macedonia) or the M 6.4 in 2019 at Durres (Albania). Seismicity is widely distributed in the area (Figure 7b). However, it has been noticed that seismic events are more frequent in the western part (Albania, western Greece, and western part of North Macedonia) and less frequent in the eastern part (Burchfiel et al., 2006). This observation is consistent with the distribution of active neotectonic faulting, which occurs as

new ruptures are created along old structures. This type of seismicity may be related to highly pressurized CO_2 that is accumulated in crustal reservoirs, and favors mechanisms of fault weakening (Miller et al., 2004). As hypothesized for the Apennine chain in Italy (Chiodini et al., 2020), that has a similar geodynamic regime, CO_2 in the western part of the South Balkan Peninsula may be continuously released from carbonates in the slab to the mantle wedge and to the lower crust (Frezzotti et al., 2009). CO_2 ascends from depth and the increasing pressure within the deep reservoirs may drive the migration toward the uppermost crustal layers (Chiodini et al., 2013). Gas exsolution from deep CO_2 reservoirs during seismic events results in an increased gas release to the atmosphere (Chiodini et al., 2020).

An example of extensive degassing through widespread cold CO_2-rich manifestations is the Pelagonian basin (Prilep-Bitola-Florina basin). This is an NNW-SSE oriented intra-montane graben (Arsovski, 1997) sited in the southern part of the country, which extends for more than 100 km from Prilep in North Macedonia to Kozani in Greece. Here, several CO_2-rich mineral springs and wells are found, resulting from the migration of CO_2 from depth to the surface along faults and fracture zones (Koukouzas et al., 2015). Although great amounts of CO_2 are extracted from companies in both countries, the presence of extensive natural CO_2 accumulations is well documented only on the Greek side (D'Alessandro et al., 2011; Gemeni et al., 2015; Karakatsanis et al., 2007; Pearce et al., 2004; Ziogou et al., 2013). No data have been published for North Macedonia. Thus, the gas manifestations collected in the Bitola basin during this work represent the first geochemical evidence of CO_2 degassing for this area (Figure S1b in Supporting Information S1).

The dominant gas species at the Vardar suture undergo a notable shift toward the east, transitioning to a predominantly N_2 composition (Figure 7a; Figure S5 in Supporting Information S1) and are characterized by higher He content (Figure S6 in Supporting Information S1). These features can be ascribable both (a) to the lithology of their reservoirs, whose basement is characterized by Precambrian and Cambrian metamorphic rocks, which were strongly deformed during the formation of Variscan orogenic belt, and by several intrusions of granitic rocks (Arsovski, 1997; Schmid et al., 2020; Wang et al., 2024), and (b) to CO_2 loss through secondary processes within the reservoir and/or during gas ascent (Daskalopoulou et al., 2019; Minissale et al., 2023; Randazzo et al., 2021). The N_2-dominant composition of the thermal gas manifestations is likely caused by CO_2 removal, for example, precipitation of carbonate minerals, preferential dissolution of CO_2 in water compared to other less soluble volatiles. The high He content, together with its low isotopic ratio, indicates a long residence time of the circulating waters within the crust, where granitic intrusive and metamorphic formations, being enriched in U and Th, produce abundant He by radiogenic decay, increasing the ^4He content in the parent fluids. A similar situation is present in the Himalayan belt, where the sutures divide the purely crustal He of the Himalayan orogen from the mantle helium of the Tibet plateau (Hao et al., 2023; Klemperer et al., 2022; Li et al., 2024). Gas manifestations on the Tibet plateau are related to an extensional regime, where volatiles derived from enriched mantle wedge (CO_2 and ^3He), subducted Indian slab-carbonate (CO_2), metamorphic decarbonation reactions (CO_2) and radiogenic decay (^4He) within the crust (Hao et al., 2023).

Additionally, the geographical distribution of the geothermal fields has to be taken into account. The Vardar and the Serbo-Macedonian zones are characterized by a positive geothermal anomaly (Gorgieva et al., 2000), which is likely associated with Cenozoic volcanic activity that occurred throughout the Balkan Peninsula, following a NW-SE trending belt (Boev & Yanev, 2001; Cvetkovic et al., 2016; Molnár et al., 2022; Yanev et al., 2008). During the Late Miocene—Pliocene period, volcanism in Macedonia occurred within the Vardar zone. This resulted in the development of small-volume centers along main fault lines and/or boundaries of geotectonic units (Molnár et al., 2022). These contribute to the increased heat flow, together with radiogenic decay in the local granitoid intrusions. Exception is the Debar geothermal field, located at the border region between Albania and North Macedonia, where several hot water springs are located along an active fault on the east side of the Debar half graben (Dumurdzanov et al., 2005). Unlike the other geothermal fields, the Debar geothermal system is linked to the Peshkopia geotectonic zone (Frashëri et al., 2004). This is likely associated with deep faults at the periphery of a Triassic gypsum diapir, which represents a high thermal conductivity body (Kodhelaj, 2018).

Summing up, North Macedonia has a complex geological history and presents some of the most important structures of the Alpine-Himalayan orogenic activity. Consequently, it can be considered as one of the most active tectonic-related geogenic carbon degassing hot-spots of the Balkan peninsula.

Data Availability Statement

The data used in this study are available at EarthChem Library via Li Vigni et al. (2025).

Acknowledgments
This research was funded by Alfred P. Sloan Foundation (Deep Carbon Observatory Grant 10881-TDB "Improving the estimation of tectonic carbon flux"), by the European Social Fund (PO FSE Sicilia, 2014–2020) in the frame of the project "Metodi di controllo geochimico e geofisico dei fenomeni naturali sul campo ed in laboratorio" (CUP: G77B17000200009), by the Italian Ministero Istruzione Università e Ricerca (MIUR, under Grant PRIN2017-2017LMNLAW) and was supported by the European Union and the State of Hungary, co-financed by the European Regional Development Fund in the project of GINOP-2.3.2-15-2016-00009 "ICER." Fieldwork was carried out under Research permits Nos. UP1-11/1–691/2019 and UP1-11/1–1829/2019 issued by the Ministry of Environment and Physical Planning of the Republic of North Macedonia and Research permit No. 14–190/3, issued by the Geological Survey of the Republic of North Macedonia. We thank Ivica Milevski for support in obtaining research permits, and Vladimir Jugovski, Pece Veljanoski, Mimoza Kočovska, Peco Ristevski, Pavle Gjorgoski and others for help in accessing the sampling sites. We thank the two reviewers for their suggestions.

References

Allard, P., Maiorani, A., Tedesco, D., Cortecci, G., & Turi, B. (1991). Isotopic study of the origin of sulfur and carbon in Solfatara fumaroles, Campi Flegrei caldera. *Journal of Volcanology and Geothermal Research*, *48*(1–2), 139–159. https://doi.org/10.1016/0377-0273(91)90039-3

Arsovski, M. (1997). Tectonic of Macedonia. *Faculty of Geology and Mining. Stip*, 306. (in Macedonian).

Baines, S. J., & Worden, R. H. (2004). Geological storage of carbon dioxide. *Geological Society, London, Special Publications*, *233*, 1–6. https://doi.org/10.1144/GSL.SP.2004.233.01.01

Ballentine, C. J., & Burnard, P. (2002). Production, release and transport of noble gases in the continental crust. *Reviews in Mineralogy and Geochemistry*, *47*(1), 481–538. https://doi.org/10.2138/rmg.2002.47.12

Barnes, I., Irwin, W. P., & White, D. E. (1978). Global distribution of carbon dioxide discharges and major zones of seismicity. *US Geological Survey, Water Resources Division*. https://doi.org/10.3133/wri7839

Barry, P. H., Negrete-Aranda, R., Spelz, R. M., Seltzer, A. M., Bekaert, D. V., Virrueta, C., & Kulongoski, J. T. (2020). Volatile sources, sinks and pathways: A helium-carbon isotope study of Baja California fluids and gases. *Chemical Geology*, *550*, 119722. https://doi.org/10.1016/j.chemgeo.2020.119722

Bega, Z., & Soto, J. I. (2017). The Ionian fold-and-thrust belt in central and southern Albania: A petroleum province with Triassic evaporites. In J. I. Soto, J. F. Flinch, & G. Tari (Eds.), *Permo-triassic salt province of Europe, North Africa and the Atlantic Margin. Tectonics and Hydrocarbon Potential* (pp. 517–539). Elsevier. https://doi.org/10.1016/B978-0-12-809417-4.00025-2

Berner, R. A., & Lasaga, A. C. (1989). Modelling the geochemical carbon cycle. *Scientific American*, *260*(3), 74–81. https://doi.org/10.1038/scientificamerican0389-74

Boev, B., & Yanev, Y. (2001). Tertiary magmatism within the Republic of Macedonia: A review. *Acta Vulcanologica*, *13*, 57–72.

Boykova, A. (1999). Moho discontinuity in Central Balkan Peninsula in the light of geostatistical structural analysis. *Physics of the Earth's and Planetary Interiors*, *114*(1–2), 49–58. https://doi.org/10.1016/S0031-9201(99)00045-X

Brantley, S. L., & Koepenick, K. W. (1995). Measured carbon dioxide emissions from Oldoinyo Lengai and the skewed distribution of passive volcanic fluxes. *Geology*, *23*(10), 933–936. https://doi.org/10.1130/0091-7613(1995)023<0933:MCDEFO>2.3.CO;2

Bräuer, K., Geissler, W. H., Kämpf, H., Niedermann, S., & Rman, N. (2016). Helium and carbon isotope signatures of gas exhalations in the westernmost part of the Pannonian Basin (SE Austria/NE Slovenia): Evidence for active lithospheric mantle degassing. *Chemical Geology*, *422*, 60–70. https://doi.org/10.1016/j.chemgeo.2015.12.016

Brune, S., Williams, S., & Müller, D. (2017). Potential links between continental rifting, CO_2 degassing and climate change through time. *Nature Geoscience*, *10*, 941–947. https://doi.org/10.1038/s41561-017-0003-6

Burchfiel, B. C., Nakov, R., Dumurdžanov, N., Papanikolaou, D., Tzankov, T., Serafimovski, T., et al. (2008). Evolution and dynamics of the Cenozoic tectonics of the South Balkan extensional system. *Geosphere*, *4*(6), 919–938. https://doi.org/10.1130/GES00169.1

Burchfiel, B. C., Todosov, A., King, R. W., Kotzev, V., Dumurdjanov, N., Sarafinovski, T., & Nurce, B. (2006). GPS results for Macedonia and its importance for the tectonics of the Southern Balkan extensional regime. *Tectonophysics*, *413*(3–4), 239–248. https://doi.org/10.1016/j.tecto.2005.10.046

Burton, M. R., Sawyer, G. M., & Granieri, D. (2013). Deep carbon emissions from volcanoes. In R. M. Hazen, A. P. Jones, & J. A. Baross (Eds.). *Carbon in Earth. Reviews in mineralogy and Geochemistry* (Vol. 75(1), pp. 323–354). https://doi.org/10.2138/rmg.2013.75.11

Buttita, D., Caracausi, A., Chiaraluce, L., Favara, R., Gasparo Morticelli, M., & Sulli, A. (2020). Continental degassing of helium in an active tectonic setting (northern Italy): The role of seismicity. *Scientific Reports*, *10*(1), 162. https://doi.org/10.1038/s41598-019-55678-7

Capasso, G., & Inguaggiato, S. (1998). A simple method for the determination of dissolved gases in natural waters. An application to thermal waters from Vulcano Island. *Applied Geochemistry*, *13*(5), 631–642. https://doi.org/10.1016/S0883-2927(97)00109-1

Caracausi, A., Buttita, D., Picozzi, M., Paternoster, M., & Stabile, T. A. (2022). Earthquakes control the impulsive nature of crustal helium degassing to the atmosphere. *Nature Communications, Earth & Environment*, *3*, 224. https://doi.org/10.1038/s43247-022-00549-9

Caracausi, A., & Sulli, A. (2019). Outgassing of mantle volatiles in compressional tectonic regime away from volcanism: The role of continental delamination. *Geochemistry, Geophysics, Geosystems*, *20*(4), 2007–2020. https://doi.org/10.1029/2018GC008046

Chiodini, G., Caliro, S., Cardellini, C., Frondini, F., Inguaggiato, S., & Matteucci, F. (2011). Geochemical evidence for and characterization of CO_2 rich gas sources in the epicentral area of the Abruzzo 2009 earthquakes. *Earth and Planetary Science Letters*, *274*(3–4), 372–379. https://doi.org/10.1016/j.epsl.2011.02.016

Chiodini, G., Cardellini, C., Caliro, S., Chiarabba, C., & Frondini, F. (2013). Advective heat transport associated with regional Earth degassing in central Apennine (Italy). *Earth and Planetary Science Letters*, *373*, 65–74. https://doi.org/10.1016/j.epsl.2013.04.009

Chiodini, G., Cardellini, C., Di Luccio, F., Selva, J., Frondini, F., Caliro, S., et al. (2020). Correlation between tectonic CO_2 Earth degassing and seismicity is revealed by a 10-year record in the Apennines, Italy. *Science Advances*, *6*(35), eabc2938. https://doi.org/10.1126/sciadv.abc2938

Chiodini, G., Frondini, F., Kerrick, D. M., Rogie, J., Parello, F., Peruzzi, L., & Zanzari, A. R. (1999). Quantification of deep CO_2 fluxes from central Italy: Examples of carbon balance for regional aquifers and soil degassing. *Chemical Geology*, *159*(1–4), 205–222. https://doi.org/10.1016/S0009-2541(99)00030-3

Chiodini, G., Frontini, F., Cardellini, C., Parello, F., & Peruzzi, L. (2000). Rate of diffuse carbon dioxide Earth degassing estimated from carbon balance of regional aquifers: The case of central Apennine, Italy. *Journal of Geophysical Research*, *105*(B4), 8423–8434. https://doi.org/10.1029/1999JB900355

Clark, I. D., & Fritz, P. (1997). *Environmental isotopes in hydrogeology* (2nd ed., pp. 210–212). CRC Press. https://doi.org/10.1201/9781482242911

Cvetkovic, V., Prelevic, D., & Schmid, S. (2016). Geology of south-eastern Europe. In P. Papic (Ed.), *Mineral and thermal waters of southeastern Europe. Environmental Earth science*. Springer. https://doi.org/10.1007/978-3-319-25379-4_1

D'Alessandro, W., Bellomo, S., Brusca, L., Karakazanis, S., Kyriakopoulos, K., & Liotta, M. (2011). The impact on water quality of the high carbon dioxide contents of the groundwater in the area of Florina (N. Greece). In N. Lambrakis, G. Stournaras, & K. Katsanou (Eds.), *Advances in the research of aquatic environment* (Vol. 2, pp. 135–143). Springer. https://doi.org/10.1007/978-3-642-24076-8_16

D'Alessandro, W., Daskalopoulou, K., Calabrese, S., & Bellomo, S. (2018). Water chemistry and abiogenic methane content of a hyperlkaline spring related to serpentinization in the Argolida ophiolite (Ermioni, Greece). *Marine and Petroleum Geology*, *89*, 185–193. https://doi.org/10.1016/j.marpetgeo.2017.01.028

D'Alessandro, W., Li Vigni, L., Gagliano, A. L., Calabrese, S., Kyriakopoulos, K., & Daskalopoulou, K. (2020). CO_2 release to the atmosphere from thermal springs of Sperchios Basin and northern Euboea (Greece). The contribution of "hidden" degassing. *Applied Geochemistry*, *119*, 104660. https://doi.org/10.1016/j.apgeochem.2020.104660

D'Angeli, I. M., Parise, M., Vattano, M., Madonia, G., Galdenzi, S., & De Waele, J. (2019). Sulfuric acid caves of Italy: A review. *Geomorphology*, *333*, 105–122. https://doi.org/10.1016/j.geomorph.2019.02.025

Daskalopoulou, K., Calabrese, S., Gagliano, A. L., & D'Alessandro, W. (2019). Estimation of the geogenic carbon degassing of Greece. *Applied Geochemistry*, *106*, 60–74. https://doi.org/10.1016/j.apgeochem.2019.04.018

Daskalopoulou, K., Calabrese, S., Grassa, F., Kyriakopoulos, K., Parello, F., Tassi, F., & D'Alessandro, W. (2018). Origin of methane and light hydrocarbons in natural fluid emissions: A key study from Greece. *Chemical Geology*, *479*, 286–301. https://doi.org/10.1016/j.chemgeo.2018.01.027

Drogreška, K. (2018). *Use of the dislocation theory in defining the epicentral areas and tectonic conditions in the territory of the republic of Macedonia*. Skopje (PhD thesis). Ss. Cyril and Methodius University.

Du, J., Cheng, W., Zhang, Y., Jian, C., Guan, Z., Liu, W., & Bai, L. (2006). Helium and Carbon isotopic compositions of thermal springs in earthquake zone of Sichuan, Southwestern China. *Journal of Asian Earth Sciences*, *26*(5), 533–539. https://doi.org/10.1016/j.jseaes.2004.11.006

Dumurdzanov, N., Serafimovski, T., & Burchfiel, B. C. (2004). Evolution of the Neogene-Pleistocene basins of Macedonia. *Geol Soc Am Digit Map Chart Ser*, *1*, 1–20. https://doi.org/10.1130/2004-dumurdzanov-macedonia

Dumurdzanov, N., Serafimovski, T., & Burchfiel, B. C. (2005). Cenozoic tectonics of Macedonia and its relation to the South Balkan extensional regime. *Geosphere*, *1*(1), 1–22. https://doi.org/10.1130/GES00006.1

Etiope, G., Christodoulou, D., Kordella, S., Marinaro, G., & Papatheodorou, G. (2013). Offshore and onshore seepage of thermogenic gas at Katakolo Bay (Greece). *Chemical Geology*, *347*, 115–126. https://doi.org/10.1016/j.chemgeo.2012.08.011

Evans, M. J., Derry, L. A., & France-Lanord, C. (2008). Degassing of metamorphic carbon dioxide from the Nepal Himalaya. *Geochemistry, Geophysics, Geosystems*, *9*(4), Q04021. https://doi.org/10.1029/2007GC001796

Faulker, D. R., Jackson, C. A. L., Lunn, R. J., Schlische, R. W., Shipton, Z. K., Wibberley, C. A. J., & Withjack, M. O. (2010). A review of recent developments concerning the structure, mechanics and fluid flow properties of fault zones. *Journal of Structural Geology*, *32*(11), 1557–1575. https://doi.org/10.1016/j.jsg.2010.06.009

Fischer, T. P., Arellano, S., Carn, S., Aiuppa, A., Galle, B., Allard, P., et al. (2019). The emissions of CO_2 and other volatiles from the world's subaerial volcanoes. *Scientific Reports*, *9*(1), 18716. https://doi.org/10.1038/s41598-019-54682-1

Fischer, T. P., Giggenbach, W. F., Sano, Y., & Williams, S. N. (1998). Fluxes and sources of volatiles discharged from Kudryavy, a subduction zone volcano, Kurile Islands. *Earth and Planetary Science Letters*, *160*(1–2), 81–96. https://doi.org/10.1016/S0012-821X(98)00086-7

Foster, G., Royer, D., & Lunt, D. (2017). Future climate forcing potentially without precedent in the last 420 million years. *Nature Communications*, *8*(1), 14845. https://doi.org/10.1038/ncomms14845

Frashëri, A., & Čermak, V. (2004). *The geothermal atlas of Albania* (pp. 65–89). Sh. BLU. Tirana.

Frashëri, A., Nishani, P., Bushati, S., & Hyseni, A. (1996). Relationship between tectonic zone of the Albanides, based on results of geophysical studies. In P. A. Ziegler & F. Horwath (Eds.), *Peri-tethys Memoir 2: Structure and Prospects of Alpine basins and Forelands* (Vol. 170, pp. 485–511). Mem. Musee Hist. Nat.

Frezzotti, M. L., Peccerillo, A., & Panza, G. (2009). Carbonate metasomatism and CO_2 lithosphere-asthenosphere degassing beneath the Western Mediterranean: An integrated model arising from petrological and geophysical data. *Chemical Geology*, *262*(1–2), 108–120. https://doi.org/10.1016/j.chemgeo.2009.02.015

Frondini, F., Cardellini, C., Caliro, S., Beddini, G., Rosiello, A., & Chiodini, G. (2019). Measuring and interpreting CO_2 fluxes at regional scale: The case of the Apennines, Italy. *Journal of the Geological Society*, *176*(2), 408–416. https://doi.org/10.1144/jgs2017-169

Gautheron, C., Moreira, M., & Allègre, C. (2005). He, Ne and Ar composition of the European lithospheric mantle. *Chemical Geology*, *217*, 97–112. https://doi.org/10.1016/j.chemgeo.2004.12.009

Gemeni, V., Vasilatos, C., Koukouzas, N., & Kanellopoulos, C. (2015). Geochemical consequences in shallow aquifers from the long-term presence of CO_2 in a natural field: The case of Florina Basin, W. Macedonia, Greece. *Greenhouse Gases: Science and Technology*, *6*(4), 450–469. https://doi.org/10.1002/ghg.1574

Giggenbach, W. F. (1997). Relative importance of thermodynamic and kinetic processes in governing the chemical and isotopic composition of carbon gases in high-heatflow sedimentary basins. *Geochimica et Cosmochimica Acta*, *61*(17), 3763–3785. https://doi.org/10.1016/S0016-7037(97)00171-3

Giggenbach, W. F. (1980). Geothermal gas equilibria. *Geochimica et Cosmochimica Acta*, *44*(12), 2021–2032. https://doi.org/10.1016/0016-7037(80)90200-8

Giggenbach, W. F. (1987). Redox processes governing the chemistry of fumarolic gas discharges from White Island, New Zealand. *Applied Geochemistry*, *2*, 143–161. https://doi.org/10.1016/0883-2927(87)90030-8

Giggenbach, W. F. (1996). Chemical composition of volcanic gases. In R. Scarpa & R. Tilling (Eds.), *Monitoring and mitigation of volcanohazard* (pp. 222–256). Springer-Verlag.

Giggenbach, W. F., Gonfiantini, R., Jangi, B. L., & Truesdell, A. H. (1983). Isotopic and chemical composition of Parbaty Valley geothermal discharges, NW-Himalaya. *Geothemics*, *12*(2–3), 199–222. https://doi.org/10.1016/0375-6505(83)90030-5

Gilfillan, S. M. V., Sherwood Lollar, B., Holland, G., BlagBurn, D., Stevens, S., Schoell, M., et al. (2009). Solubility trapping in formation water as dominant CO2 sink in natural gas fields. *Nature*, *458*(7238), 614–618. https://doi.org/10.1038/nature07852

Gorgieva, M. (1989). *Chemical geothermometers and mineral equilibria of some hot waters in Yugoslavia* (p. 61pp). Report UNU Geothermal Training Programme.

Gorgieva, M., Gorgiev, D., Popovski, K., Dimitov, K., & Manasov, S. (2000). Inferred section of the main (low-temperature) geothermal systems in the Republic of Macedonia. *Proceedings World Geothermal Congress 2000*.

Grigoriadis, V., Tziavos, I., Tsokas, G., & Stampolidis, A. (2016). Gravity data inversion for Moho depth modeling in the Hellenic area. *Pure and Applied Geophysics*, *173*(4), 1223–1241. https://doi.org/10.1007/s00024-015-1174-y

Haendel, D., Mohle, K., Nitzsche, H. M., Stihl, G., & Wand, U. (1986). Isotopic variations of the fixed nitrogen in metamorphic rocks. *Geochimica et Cosmochimica Acta*, *50*, 749–758. https://doi.org/10.1016/0016-7037(86)90351-0

Hao, Y., Kuang, X., Feng, Y., Wang, Y., Zhou, H., & Zheing, C. (2023). Discovery and genesis of helium-rich geothermal fluids along the India-Asia continental convergent margin. *Geochimica et Cosmochimica Acta*, *360*, 175–191. https://doi.org/10.1016/j.gca.2023.09.011

Heydari, E. (1997). The role of burial diagenesis in hydrocarbon destruction and H_2S accumulation, Upper Jurassic Smackover formation, Black Creek Field, Mississippi. *The American Association of Petroleum Geologists Bulletin*, *81*, 26–45.

Holland, G., & Gilfillan, S. (2013). Application of noble gases to the viability of CO_2 storage. In P. Burnard (Ed.), *The noble gases as geochemical tracers. Advances in isotope geochemistry* (pp. 177–223). Springer. https://doi.org/10.1007/978-3-642-28836-4_8

Hunt, J. A., Zafu, A., Mather, T. A., Pyle, D. M., & Barry, P. H. (2017). Spatially variable CO_2 degassing in the main Ethiopian rift: Implications for magma storage, volatile transport, and rift-related emissions. *Geochemistry, Geophysics, Geosystems*, *18*(10), 3714–3737. https://doi.org/10.1002/2017/2017GC006975

Hunt, J. M. (1996). *Petroleum geochemistry and geology*. W.H. Freeman and Company.

Iloski, G., Ivanovski, G., & Oracheski, S. (1957). Извештај за сулфурните појави кај с.Косел-Охридско, Биро за геолошки истражувања – Охрид. In *Report on sulfur phenomena in the village of Kosel-Ohrid*. Bureau for Geological Research – Ohrid. (*in Macedonian*).

Inguaggiato, S., & Rizzo, A. (2004). Dissolved helium isotope ratios in groundwaters: A new technique based on gas-water re-equilibration and its application to stromboli volcanic system. *Applied Geochemistry*, *19*(5), 665–673. https://doi.org/10.1016/j.apgeochem.2003.10.009

Irwin, W. P., & Barnes, I. (1980). Tectonic relations of carbon dioxide discharges and earthquakes. *Journal of Geophysical Research*, *85*(B6), 3115–3121. https://doi.org/10.1029/JB085iB06p03115

Italiano, F., Yüce, G., Uysal, I. T., Gasparon, M., & Morelli, G. (2014). Insights into mantle-type volatiles contribution from dissolved gases in artesian waters of the Great Artesian Basin, Australia. *Chemical Geology*, *378–379*, 75–88. https://doi.org/10.1016/j.chemgeo.2014.04.013

Jančev, S., Pezdič, J., Szaran, J., & Halas, S. (1999). Characteristics of sulphate occurrences near Kosovrasti, Macedonia. *RMZ*, *46*(3), 501–508.

Javoy, M., Pineau, F., & Demaiffe, D. (1984). Nitrogen and carbon isotopic composition in the diamonds of Mbuji Mayi (Zaire). *Earth and Planetary Science Letters*, *68*(3), 399–411. https://doi.org/10.1016/0012-821X(84)90125-0

Jenden, P. D., Hilton, D. R., Kaplan, I. R., & Craig, H. (1993). Abiogenic hydrocarbons and mantle helium in oil and gas fields. In D. G. Howell (Ed.), *The future of energy gases: US Geol. Surv. Profes. Paper* (Vol. 1570, pp. 31–56).

Jenden, P. D., Kaplan, I. R., Poreda, R. J., & Craig, H. (1988). Origin of nitrogen-rich natural gases in the California Great Valley: Evidence from helium, carbon and nitrogen isotope ratios. *Geochimica et Cosmochimica Acta*, *52*(4), 851–861. https://doi.org/10.1016/0016-7037(88)90356-0

John, T., Gussone, N., Podladchikov, Y. Y., Bebout, G. E., Dohmen, R., Halama, R., et al. (2012). Volcanic arcs fed by rapid fluid flow through subducting slabs. *Nature Geoscience Letters*, *5*(7), 489–492. https://doi.org/10.1038/ngeo1482

Jolivet, L., & Brun, J. P. (2010). Cenozoic geodynamic evolution of the Aegean. *International Journal of Earth Sciences*, *99*(1), 109–138. https://doi.org/10.1007/s00531-008-0366-4

Karakatsanis, S., Koukouzas, N., Pagonas, M., & Zelilidis, A. (2007). Preliminary sedimentological results indicate a new detailed stratigraphy for the Florina sedimentary basin and relate them with CO_2 presence. *Bull. Geol. Soc. Greece 40, Proc. 11th Internat. Congr*, *40*(1), 76. https://doi.org/10.12681/bgsg.16337

Kerrick, D. M. (2001). Present and past nonanthropogenic CO_2 degassing from the solid earth. *Reviews of Geophysics*, *39*(4), 565–585. https://doi.org/10.1029/2001RG000105

Kerrick, D. M., McKibben, M. A., Seward, T. M., & Caldeira, K. (1995). Convective hydrothermal CO_2 emission from high heat flow regions. *Chemical Geology*, *121*(1–4), 285–293. https://doi.org/10.1016/0009-2541(94)00148-2

King, C. Y. (1986). Gas geochemistry applied to earthquakes prediction: An overview. *Journal of Geophysical Research*, *91*(B12), 12269–12281. https://doi.org/10.1029/JB091iB12p12269

Kipfer, R., Aeschbach-Hertig, W., Peeters, F., & Stute, M. (2002). Noble gases in lakes and ground waters. *Reviews in Mineralogy and Geochemistry*, *47*(1), 615–700. https://doi.org/10.2138/rmg.2002.47.14

Kis, B. M., Caracausi, A., Palcsu, L., Baciu, C., Ionescu, A., Futò, I., et al. (2019). Noble gas and carbon isotope systematics at the seemingly inactive Ciomadul volcano (Eastern-Central Europe, Romania): Evidence for volcanic degassing. *Geochemistry, Geophysics, Geosystems*, *20*(6), 3019–3043. https://doi.org/10.1029/2018GC008153

Kis, B. M., Ionescu, A., Cardellini, C., Harangi, S., Baciu, C., Caracausi, A., & Viveiros, F. (2017). Quantification of carbon dioxide emissions of Ciomadul, the youngest volcano of the Carpathian-Pannonian Region (Eastern-Central Europe, Romania). *Journal of Volcanology and Geothermal Research*, *341*, 119–130. https://doi.org/10.1016/j.jvolgeores.2017.05025

Kleine, B. I., Skelton, A. D. L., Huet, B., & Pitcairn, I. K. (2014). Preservation of blueschist-facies minerals along a shear zone by coupled metasomatism and fast-flowing CO2-bearing fluids. *Journal of Petrology*, *55*(10), 1905–1939. https://doi.org/10.1093/petrology/egu045

Kleine, B. I., Zhao, Z., & Skelton, A. D. L. (2016). Rapid fluid flow along fractures at greenschist facies conditions on Syros, Greece. *American Journal of Science*, *316*(2), 169–201. https://doi.org/10.2475/02.2016.03

Klemperer, S. L., Zhao, P., Whyte, C. J., Darrah, T. H., Crossey, L. J., Karlstrom, K. E., et al. (2022). Limited underthrusting of India below Tibet: $^3He/^4He$ analysis of thermal springs locates the mantle suture in continental collision. *Proceedings of the National Academy of Sciences*, *119*(12), e2113877119. https://doi.org/10.1073/pnas.2113877119

Kodhelaj, N. (2018). *Geothermal energy and its use in Albania*. LAMBERT Academic Publishing.

Kolios, N., Innocenti, F., Manetti, P., Peccerillo, A., & Giuliani, O. (1980). The Pilocene volcanism of the Voras mts (Central Macedonia, Greece). *Bulletin of Volcanology*, *43*(3), 553–568. https://doi.org/10.1007/BF02597692

Kossmat, F. (1924). Geologie der zentralen Balkanhalbinsel: Mit einer Übersicht des dinarischen Gebirgsbaus. *Die Kriegsschauplätze 1914–1918 geologisch dargestellt*, *12*, 198.

Koukouzas, N., Tasianas, A., Gemeni, V., Alexopoulos, D., & Vasilatos, C. (2015). Geological modelling for investigating CO_2 emissions in Florina Basin, Greece. *Open Geosciences*, *7*(1), 20150039. https://doi.org/10.1515/geo-2015-0039

Lee, J. Y., Marti, K., Severinghaus, J. P., Kawamura, K., Yoo, H. S., Lee, J. B., & Kim, J. S. (2006). A redetermination of the isotopic abundances of atmospheric Ar. *Geochimica et Cosmochimica Acta*, *70*(17), 4507–4512. https://doi.org/10.1016/j.gca.2006.06.1563

Lévy, D., Boka-Mene, M., Meshi, A., Fejza, I., Guermont, T., Hauville, B., & Pelisser, N. (2023). Looking for natural hydrogen in Albania and Kosova. *Frontiers of Earth Science*, *11*, 1167634. https://doi.org/10.3389/feart.2023.1167634

Lewicki, J., & Brantley, S. L. (2000). CO_2 degassing along the san Andreas fault, Parkfield, California. *Geophysical Research Letters*, *27*(1), 5–8. https://doi.org/10.1029/1999GL008380

Li, J., Gou, Z., Zhang, M., Zhao, W., Dingwell, D. B., Zheng, G., et al. (2024). Deep-sourced CO_2 emissions from the eastern Himalaya syntaxis and the Tengchong volcanic field, southeast Tibet. *Chemical Geology*, *645*, 121888. https://doi.org/10.1016/j.chemgeo.2023.121888

Liotta, M., & Martelli, M. (2012). Dissolved gases in brackish thermal waters: An improved analytical method. *Geofluids*, *12*(3), 236–244. https://doi.org/10.1111/j.1468-8123.2012.00365.x

Li Vigni, L., Cardellini, C., Temovski, M., Ionescu, A., Molnar, K., Palcsu, L., et al. (2022). Duvalo "volcano" (North Macedonia): A purely tectonic-related CO_2 degassing system. *Geochemistry, Geophysics, Geosystems*, *23*(4), E2021GC010198. https://doi.org/10.1029/2021GC010198

Li Vigni, L., Daskalopoulou, K., Calabrese, S., Parello, F., & D'Alessandro, W. (2021). Geochemical characterization of the alkaline and hyperalkaline groundwater in the Othrys Ophiolite Massif, central Greece. *Italian Journal of Geosciences*, *140*, 42–56. https://doi.org/10.3301/IJG.2020.20

Li Vigni, L., Temovski, M., Cardellini, C., Molnár, K., Ionescu, A., Vojo, M., et al. (2025). Chemical and isotope composition of gases from North Macedonia (Balkan Peninsula - Southern Europe), version 1.0. *Interdisciplinary Earth Data Alliance (IEDA)*. https://doi.org/10.60520/IEDA/113754

Machel, H. G. (2001). Bacterial and thermochemical sulfate reduction in diagenetic settings – Old and new insights. *Sedimentary Geology*, *140*(1–2), 143–175. https://doi.org/10.1016/S0037-0738(00)00176-7

Manzano, B. K., Fowler, M. G., & Machel, H. G. (1997). The influence of thermochemical sulfate reduction on hydrocarbon composition in Nisku reservoirs, Brazeau River area, Alberta, Canada. *Organic Geochemistry*, *27*, 507±521. https://doi.org/10.1016/S0146-6380(97)00070-3

Marini, L., & Chiodini, G. (1994). The role of carbon dioxide in the carbonate-evaporite geothermal systems of Tuscany and Latium (Italy). *Acta Volcanol*, *5*, 95–104.

Markoski, B., Jovanovski, M., & Peshevski, I. (2019). Duvalo – Dry mofette. *Kosel, Ohrid. Geomap doo, Skopje*. (in Macedonian with extended summary in English).

Marty, B., Almayrac, M., Barry, P. H., Bekaert, D. V., Broadley, M. W., Byrne, D. J., et al. (2020). An evaluation of the C/N ratio of the mantle from natural CO_2-rich gases analysis: Geochemical and cosmochemical implications. *Earth and Planetary Science Letters*, *551*(2020), 116574. https://doi.org/10.1016/j.epsl.2020.116574

Mazor, E. (1991). *Applied chemical and isotopic groundwater Hydrology* (p. 274). Open University Press.

Micevski, E., Popovski, K., Popovska-Vasilevska, S., & Kolcakovski, Z. (2007). The hydrogeothermal potential of the Vardar zone and Serbo-Macedonian mass and energetical valorization of the available geothermal resources at the territory of the Republic of Macedonian. *European Geothermal Congress, Germany, 30 May – 1 June*.

Milivojevic, M. (1993). Geothermal model of Earth's Crust and litosphere for the territory of Yugoslavia: Some tectonic implications. *Studia Geoph. et Geol*, *37*, 23–31.

Miller, S. A., Ben-Zion, Y., & Burg, J. P. (1999). A three-dimensional fluid controlled earthquake model: Behaviour and implications. *Journal of Geophysical Research*, *104*(B5), 10621–10638. https://doi.org/10.1029/1998JB900084

Miller, S. A., Collettini, C., Chiaraluce, L., Cocco, M., Barchi, M., & Kaus, B. J. (2004). Aftershocks driven by a high-pressure CO_2 source at depth. *Nature*, *427*(6976), 724–727. https://doi.org/10.1038/nature02251

Minissale, A., Vaselli, O., Marchev, P., & Tassi, F. (2023). Geochemistry of thermal springs and associated gases along the Strymon River Valley (Bulgaria and Greece). *Journal of Geochemical Exploration*, *252*, 107262. https://doi.org/10.1016/j.gexplo.2023.107262

Molnár, K., Lahitte, P., Dibacto, S., Benkó, Z., Agostini, S., Döncző, B., et al. (2022). The westernmost Late Miocene-Pliocene volcanic activity in the Vardar zone (North Macedonia). *International Journal of Earth Sciences*, *111*(3), 749–766. https://doi.org/10.1007/s00531-021-02153-2

Molnár, K., Lahitte, P., Döncző, B., Arató, R., Szepesi, J., Benkó, Z., et al. (2023). Unravelling the pre-eruptive conditions of the rhyolitic Šumovit Greben lava dome from clinopyroxene-dominant glomeroporphyritic clots. *Contributions to Mineralogy and Petrology*, *178*(11), 83. https://doi.org/10.1007/s00410-023-02066-0

Molnár, K., Temovski, M., & Palcsu, L. (2021). First noble gas results from fluid inclusions of the Late Miocene- Pleistocene Macedonian volcanics. *EGU General Assembly*. https://doi.org/10.5194/egusphere-egu21-9440

Mörner, N. K., & Etiope, G. (2002). Carbon degassing from the lithosphere. *Global and Planetary Change*, *33*(1–2), 185–203. https://doi.org/10.1016/S0921-8181(02)00070-X

Muirhead, J. D., Kattenhorn, S. A., Lee, H., Mana, S., Turrin, B. D., Fischer, T. P., et al. (2016). Evolution of upper crustal faulting assisted by magmatic volatile release during early-stage continental rift development in the East African Rift. *Geosphere*, *12*(6), 1670–1700. https://doi.org/10.1130/GES01375.1

Naunov, J. (2003). Geotermal system Geoterma. *Second conference for geothermal energy in Macedonia (Proceedings)*, 5–15.

Nieuwland, D. A., Oudmayer, B. C., & Valbona, U. (2001). The tectonic development of Albania: Explanation and prediction of structural styles. *Marine and Petroleum Geology*, *18*(1), 161–177. https://doi.org/10.1016/S0264-8172(00)00043-X

Ohmoto, H., & Lasaga, A. C. (1982). Kinetics of reactions between aqueous sulphates and sulphides in hydrothermal system. *Geochimica et Cosmochimica Acta*, *46*(10), 1727–1745. https://doi.org/10.1016/0016-7037(82)90113-2

Ozima, M., & Podosek, F. A. (2002). *Noble gas geochemistry*. Cambridge University Press. (Vol. 2, p. 286). https://doi.org/10.1017/S0016756803258349

Pearce, J. M., Czernichowski-Lauriol, I., Lombardi, S., Brune, S., Nador, A., Baker, J., et al. (2004). A review of natural CO_2 accumulations in Europe as analogues for geological sequestration. *Geological Society of London Special Publications*, *233*(1), 29–41. https://doi.org/10.1144/gsl.sp.2004.233.01.04

Peterson, D. E., Finger, K. L., Iepure, S., Mariani, S., Montanari, A., & Namiotko, T. (2013). Ostracod assemblages in the Frasassi caves and adjacent sulfidic spring and Sentino River in the northeastern Apennines of Italy. *Journal of Cave and Karst Studies*, *75*(1), 11–27. https://doi.org/10.4311/2011PA0230

Piperov, N. B., Kamensky, I. L., & Tolstikhin, I. N. (1994). Isotopes of the light noble gases in mineral waters in the eastern part of the Balkan peninsula, Bulgaria. *Geochimica et Cosmochimica Acta*, *55*(8), 1889–1898. https://doi.org/10.1016/0016-7037(94)90422-7

Popovska-Vasilevska, S., & Armenski, S. (2016). Geothermal potential of Macedonia and its utilization. In P. Papić (Ed.), *Mineral and thermal waters of southeastern Europe. Environmental Earth science* (pp. 131–146). Springer. https://doi.org/10.1007/978-3-319-25379-4_8

Randazzo, P., Caracausi, A., Aiuppa, A., Cardellini, C., Chiodini, G., Apollaro, C., et al. (2022). Active degassing of crustal CO_2 in areas of tectonic collision: A case study from the Pollino and Calabria sectors (southern Italy). *Frontiers in Earth Science*, *10*, 946707. https://doi.org/10.3389/feart.2022.946707

Randazzo, P., Caracausi, A., Aiuppa, A., Cardellini, C., Chiodini, G., D'Alessandro, W., et al. (2021). Active degassing of deeply sourced fluids in central Europe: New evidences from a geochemical study in Serbia. *Geochemistry, Geophysics, Geosystems*, *22*(11), e2021GC010017. https://doi.org/10.1029/2021GC010017

Ray, M. C., Hilton, D. R., Munoz, J., Fischer, T. P., & Shaw, A. M. (2009). The effects of volatile recycling, degassing and crustal contamination on the helium and carbon geochemistry of hydrothermal fluids from the Southern Volcanic Zone of Chile. *Chemical Geology*, *266*(1–2), 38–49. https://doi.org/10.1016/j.chemgeo.2008.12.026

Sano, Y., & Marty, B. (1995). Origin of carbon in fumarolic gas from islands arcs. *Chemical Geology*, *119*(1–4), 265–274. https://doi.org/10.1016/0009-2541(94)00097-R

Sano, Y., & Wakita, H. (1985). Geographical distribution of $^3He/^4He$ ratios in Japan: Implications for arc tectonics and incipient magmatism. *Journal of Geophysical Research*, *90*(B10), 8729–8741. https://doi.org/10.1029/JB090iB10p08729

Schmid, S. M., Fügenschuh, B., Kounov, A., Maţenco, L., Nievergelt, P., Oberhänsli, R., et al. (2020). Tectonic units of the Alpine collision zone between Eastern Alps and western Turkey. *Gondwana Research*, *78*, 308–374. https://doi.org/10.1016/j.gr.2019.07.005

Seward, T. M., & Kerrick, D. M. (1996). Hydrothermal CO_2 emissions from the Taupo volcanic zone. New Zeland. *Earth and Planetary Science Letters*, *139*(1–2), 105–113. https://doi.org/10.1016/0012-821X(96)00011-8

Sharp, Z. D., Papike, J. J., & Durakiewicz, T. (2003). The effect of thermal decarbonation on stable isotope composition of carbonates. *American Mineralogist*, *88*(1), 87–92. https://doi.org/10.2138/am-2003-0111

Spasovski, O. (2012). Potential and geochemical characteristics of geothermal resources in Eastern Macedonia. In D. Panagiotaras (Ed.), *Geochemistry – Earth's system processes* (pp. 291–322).

Stefánsson, A., Lemke, K. H., Benezeth, P., & Scott, J. (2017). Magnesium bicarbonate and carbonate interactions in aqueous solutions: An infrared spectroscopic and quantum chemical study. *Geochimica et Cosmochimica Acta*, *198*, 271–284. https://doi.org/10.1016/j.gca.2016.10.032

Stefánsson, A., Sveinbjörnsdóttir, A. E., Heinemeier, J., Arnórsson, A., Kjartansdóttir, R., & Kristmannsdóttir, H. (2016). Mantle CO_2 degassing through the Icelandic crust: Evidence from carbon isotopes in groundwater. *Geochimica et Cosmochimica Acta*, *191*, 300–319. https://doi.org/10.1016/j.gca.2016.06.038

Stewart, E. M., Ague, J. J., Ferry, J. M., Schiffries, C. M., Tao, R., Isson, T. T., & Planacsky, N. J. (2019). Carbonation and decarbonation reactions: Implications for planetary habitability. *American Mineralogist*, *104*(10), 1369–1380. https://doi.org/10.2138/am-2019-6884

Tamburello, G., Pondrelli, S., Chiodini, G., & Rouwet, D. (2018). Global-scale control of extensional tectonics on CO_2 earth degassing. *Nature Communications*, *9*(1), 4608. https://doi.org/10.1038/s41467-018-07087-z

Temovski, M., Rinyu, L., Futó, I., Molnár, K., Túri, M., Demény, A., et al. (2022). Combined use of conventional and clumped carbonate stable isotopes to identify hydrothermal isotopic alteration in cave walls. *Scientific Reports*, *12*(1), 9202. https://doi.org/10.1038/s41598-022-12929-4

Temovski, M., Turi, M., Futo, I., Braun, M., Molnàr, K., & Palcsu, L. (2021). Multi-method geochemical characterization of groundwaters from a hypogene karst system. *Hydrogeology Journal*, *29*(3), 1129–1152. https://doi.org/10.1007/s10040-020-02293-w

Thode, H. G. (1991). Sulphur isotope in nature and the environment: An overview. In H. R. Krouse & V. A. Grinenko (Eds.), *Stable isotopes — natural and anthropogenic sulphur in the environment. Scope* (Vol. 43, pp. 1–23). Wiley.

Trojanović, S. (1925). La Solfatare de Kosel. *Annales Geologiques de la Peninsule Balkanique*, *8*(1), 140–146.

Truche, L., Donzé, F.-V., Goskolli, E., Muceku, B., Loisy, C., Monnin, C., et al. (2024). A deep reservoir for hydrogen drives intense degassing in the Bulqizë ophiolite. *Science*, *383*, 618–621. https://doi.org/10.1126/science.adk9099

Velaj, T. (2015). The structural style and the hydrocarbon exploration of the subthrust in the Berati Anticlinal Belt, Albania. *Journal of Petroleum Exploration and Production Technology*, *5*(2), 123–145. https://doi.org/10.1007/s13202-015-0162-1

Wang, Z., Song, H., Chen, Y., Song, J., Hou, M., Li, Q., et al. (2024). Uranium resource of Europe: Development status, metallogenic provinces and geodynamic setting. *Energy Strategy Reviews*, *54*, 101467. https://doi.org/10.1016/j.esr.2024.101467

Werner, C., Fischer, T. P., Aiuppa, A., Edmonds, M., Cardellini, C., Carn, S., et al. (2019). Carbon dioxide emissions from subaerial volcanic regions: Two decades in review. In *Deep Carbon past to present* (pp. 188–236). Cambridge University Press. https://doi.org/10.1017/9781108677950.008

Worden, R. H., Smalley, P. C., & Oxtoby, N. H. (1996). The effects of thermochemical sulfate reduction upon formation water salinity and oxygen isotopes in carbonate reservoirs. *Geochimica et Cosmochimica Acta*, *60*(20), 3925–3931. https://doi.org/10.1016/0016-7037(96)00216-5

World Meteorological Organization (WMO). (2019). *WMO greenhouse gas Bulletin. Report no. 15*. WMO.

World Meteorological Organization (WMO). (2023). *WMO Greenhouse Gas Bulletin. Report no. 19*. WMO.

Wróblewski, W., Bella, P., Drewnik, M., Dulinski, M., Gradzinski, M., Motyka, J., et al. (2024). Mixing of endogenous CO_2 and meteoric H_2O causes extremely efficient carbonate dissolution. *Science of the Total Environment*, *936*, 173347. https://doi.org/10.1016/j.scitotenv.2024.173347

Wycherley, H., Fleet, A., & Shaw, H. (1999). Some observations on the origins of large volumes of carbon dioxide accumulations in sedimentary basins. *Marine and Petroleum Geology*, *16*(6), 489–494. https://doi.org/10.1016/S0264-8172(99)00047-1

Yanev, Y., Boev, B., Doglioni, C., Innocenti, F., Manetti, P., Pecskay, Z., et al. (2008). Late Miocene to Pleistocene potassic volcanism in the Republic of Macedonia. *Mineria y Petroleo*, *94*(1–2), 45–60. https://doi.org/10.1007/s00710-008-0009-2

Yuçe, G., Fu, C. C., D'Alessandro, W., Gulbay, A. H., Lai, C. W., Bellomo, S., et al. (2017). Geochemical characteristics of soil radon and carbon dioxide within the dead Sea Fault and Karasu Fault in the Amik basin (Hatay) Turkey. *Chemical Geology*, *469*, 129–146. https://doi.org/10.1016/j.chemgeo.2017.01.003

Zelilidis, A., Maravelis, A. G., Tserolas, P., & Konstantopoulos, P. A. (2015). An overview of the petroleum systems in the Ionian zone, onshore NW Greece and Albania. *Journal of Petroleum Geology*, *38*(3), 331–348. https://doi.org/10.1111/jpg.12614

Ziogou, F., Gemeni, V., Koukouzas, N., de Angelis, D., Libertini, S., Beaubien, S., et al. (2013). Potential environmental impacts of CO_2 leakage from the study of natural analogue sites in Europe. *Energy Procedia*, *37*, 3521–3528. https://doi.org/10.1016/j.egypro.2013.06.245